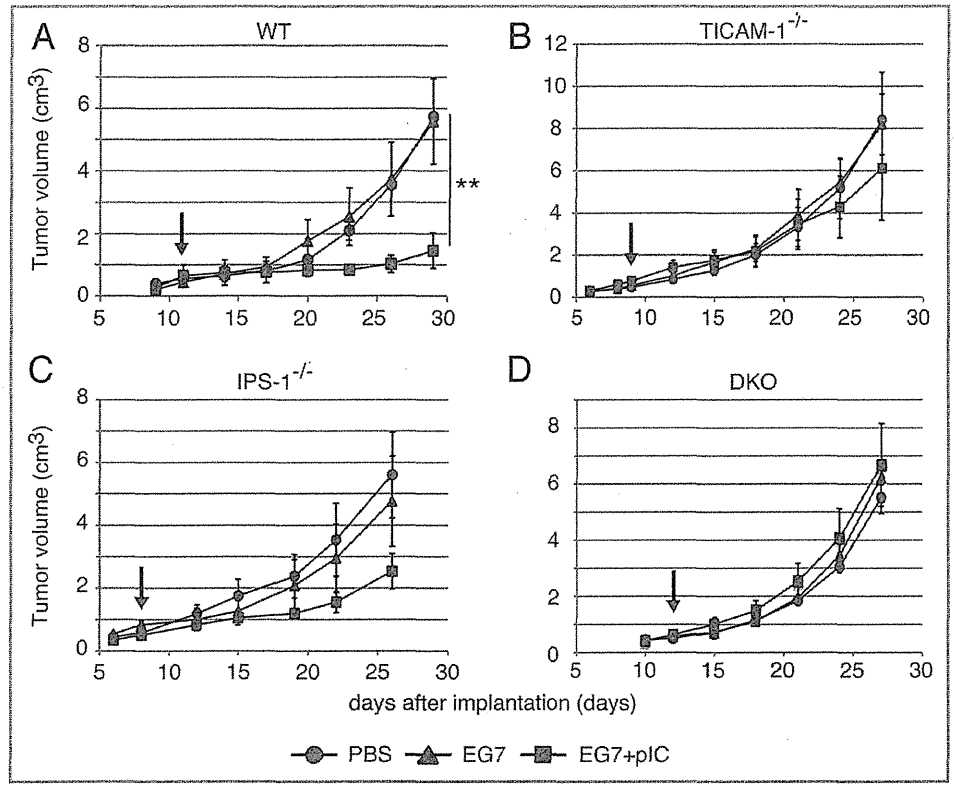


**Figure 2.** PolyI:C-induced tumor retardation is dependent on the TICAM-1 pathway. Antitumor effect of polyI:C on various KO mice were evaluated by using in vivo mouse tumor implant model. EG7 cells were inoculated to WT (A), TICAM-1$^{-/-}$ (B), IPS-1$^{-/-}$ (C) and DKO mice (D) on day 0. PBS (●), EG7 lysates (▲) or EG7 lysates + polyI:C (■) were s.c. administered around the tumor. The adjuvant therapies were started at the time indicated by the arrows and injected twice per week. Each group have 3–4 mice and error bar shows ± SEM. Data are representative of two independent experiments. **, $p < 0.01$

DC from WT mice when they were stimulated with OVA and polyI:C. Treatment of DC with OVA only did not induce upregulation of CD86 and CD40. Although the expression levels of CD86 and CD40 were a little less in CD8α$^+$ and CD8α$^-$ DC from TICAM-1$^{-/-}$ or IPS-1$^{-/-}$ mice than those from WT mice, both CD86 and CD40 were sufficiently upregulated even in the abrogation of either one pathway in polyI:C-injected mice. The CD86 and CD40 shifts were completely abolished in DKO mice (**Fig. 5A**). Thus, the TICAM-1 pathway participates in both potent co-stimulation and cross-priming, while the IPS-1 pathway mainly participates only in integral co-stimulation in myeloid DC.

We next assessed in vitro proliferation of OT-1 cells. CD8α$^+$ and CD8α$^-$ DC were prepared from PBS, polyI:C, OVA and OVA/polyI:C-treated mice, and mixed in vitro with CFSE-labeled OT-1 cells. WT, TICAM-1$^{-/-}$ and IPS-1$^{-/-}$ mice were used for this study. OT-1 proliferation was observed with CD8α$^+$ DC but not CD8α$^-$ DC when OVA + polyI:C was injected (**Fig. 5B**). Furthermore, the OT-1 proliferation barely occurred in the mixture containing TICAM-1$^{-/-}$ CD8α$^+$ DC. Thus, OT-1 proliferation is triggered by the TICAM-1 pathway in CD8α$^+$ DC. Again, IPS-1 had almost no effect on OT-1 proliferation with CD8α$^+$ DC in this setting. In the mixture, IFNγ was produced in the supernatants of WT and IPS-1$^{-/-}$ CD8α$^+$ DC but not TICAM-1$^{-/-}$ DC by stimulation with OVA + polyI:C (**Fig. 5C**). No IFNγ was produced in the supernatants of CD8α$^-$ DC even from WT mice, which results are in parallel with those of OT-1 proliferation. In any case irrespective of tumor-bearing or not, Ag, polyI:C and the TICAM-1 pathway are mandatory for CD8α$^+$ DC to cross-prime and proliferate OVA-specific CD8 T cells.

We checked the TICAM-1- or IPS-1-specific gene expressions related to Type I IFN and MHC Class I presentation using genechip and qPCR (**Fig. S6**). PolyI:C-mediated upregulation of *Tap1*, *Tap2* and *Tapbp* messages diminished in TICAM-1$^{-/-}$ BMDC (**Fig. S6A**). The levels of these genes were hardly affected in IPS-1$^{-/-}$ BMDC (data not shown). PolyI:C-mediated upregulation was observed with MDA5 (*Ifih1*) in CD8α$^-$ and CD8α$^+$ DCs (**Fig. S6B**). Surprisingly, other factors including TLR3, TICAM-1 and MAVS messages were all downregulated in response to polyI:C in CD8α$^+$ DC (**Fig. S6B**), for the reason as yet unknown.

**Effect of TLR3-mediated IFN-inducing pathway on anti-tumor CTL induction.** PolyI:C is a dsRNA analog capable of incorporating into the endosome and cytoplasm by exogenous administration in vitro.[27,28] However, no evidence has been proposed that polyI:C is internalized into the endosome of

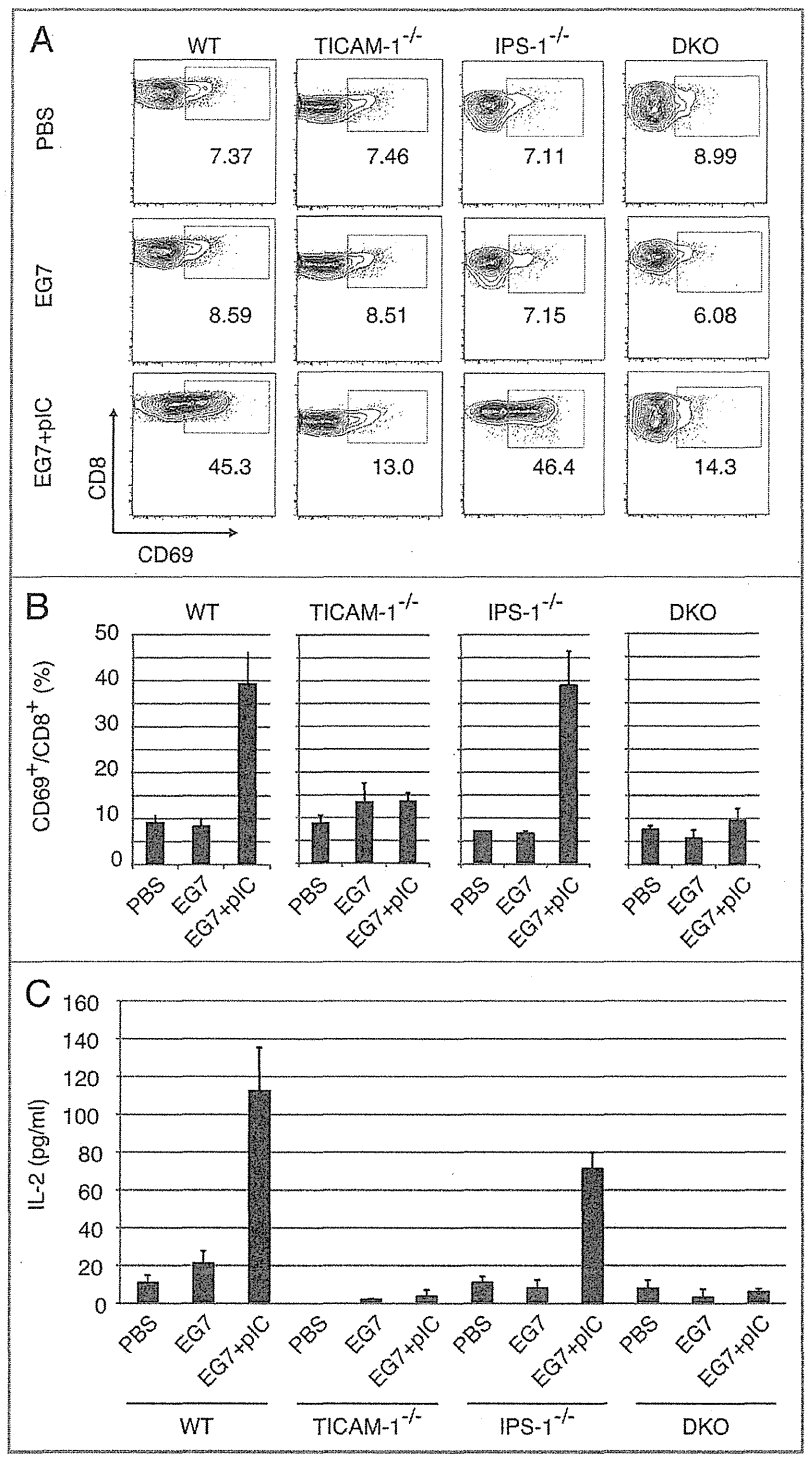


**Figure 3.** CD8 T cells in the draining LNs are activated through the TICAM-1 pathway by polyI:C. Draining inguinal LNs were harvested from tumor-bearing mice 24 h after the last treatment. LN cells were stained with CD3ε, CD8α and CD69, and the cells gated on $CD3\varepsilon^+CD8\alpha^+$ are shown (A). Spleen cells in each group of mice were stained separately, the CD8 levels in gated cells being variably distributed in FACS analyses. The average frequency of activated CD8 T cells defined by CD69 expression is shown (B). Alternatively, LN cells from the indicated mice were cultured for further 3 d in vitro and IL-2 production was measured by CBA assay (C).

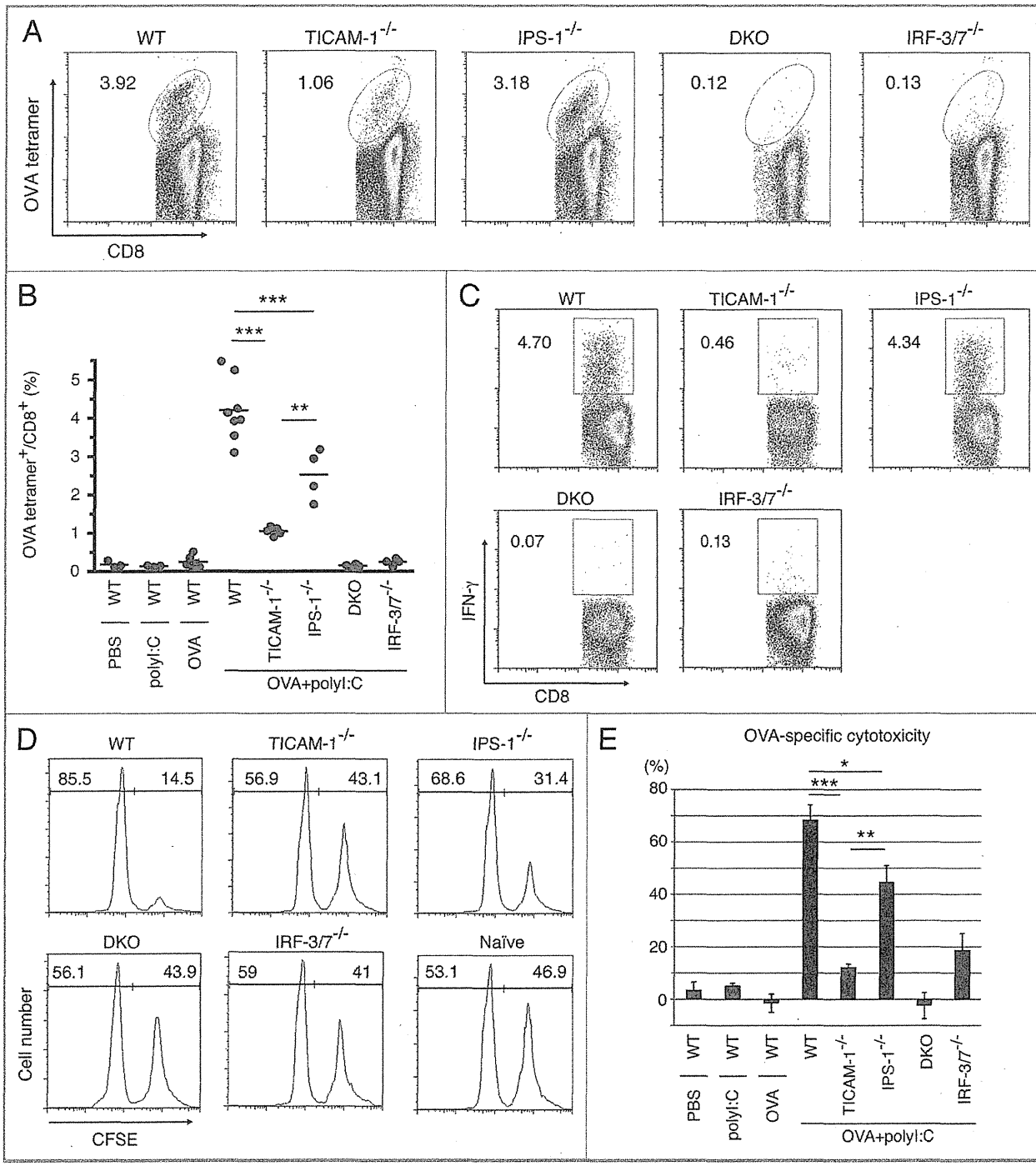


**Figure 4.** TICAM-1 and IRF-3/7 are essential for polyI:C-induced antigen-specific CTL expansion. WT, TICAM-1$^{-/-}$, IPS-1$^{-/-}$, TICAM-1/IPS-1 DKO and IRF-3/7$^{-/-}$ mice were i.p. administered with the combination of OVA and polyI:C. After 7days, splenocytes were harvested and stained with CD8α and OVA tetramer (A). The average percentages of OVA-specific CTL are shown (B). Alternatively, splenocytes were cultured in vitro in the presence of SL8 for 8 h and IFNγ production was measured by intracellular cytokine staining (C). To assess the killing activity, in vivo CTL assay was performed. The combinations of OVA and polyI:C were administered i.v. to each group of mice and 5 d later, cytotoxicity was measured (D). The data shown are collaborate or representative of at least three independent experiments. One-way analysis of variance (ANOVA) with Bonferroni's test was performed to analyze statistical significance. *, $p < 0.05$; **, $p < 0.01$; ***, $p < 0.001$.

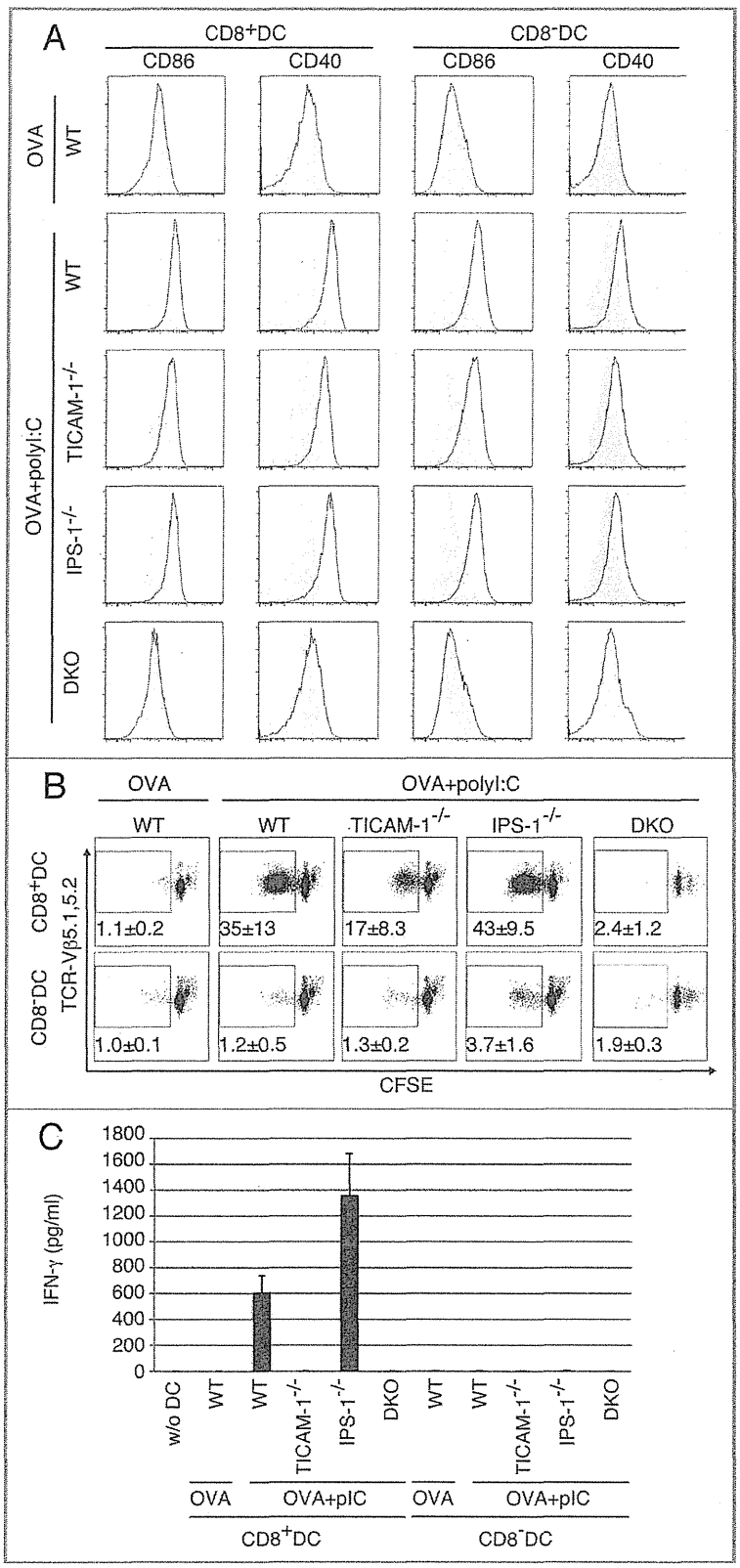


**Figure 5.** TICAM-1 in CD8α⁺ DC is more important than IPS-1 in polyI:C-induced cross-priming. OVA and polyI:C were administered i.v. and 4 h later, CD8α⁺ and CD8α⁻ DC were isolated from the spleen. CD86 and CD40 expressions were determined by FACS (A). Filled gray and black line show isotype control and target expression, respectively. Alternatively, CD8α⁺ and CD8α⁻ DC were co-cultured with CFSE-labeled RAG2$^{-/-}$/OT-1 T cells for 3 d. The cross-priming activity of each DC subset was determined with sequential dilution of CFSE (B) and IFNγ production (C). IFNγ was measured by CBA assay. The data shown are representative of two independent experiments. Err bar shows SD.

CD8α⁺ DC where TLR3 is expressed in vivo. Peritoneal (PEC) Mf and bone marrow-derived DC[22] usually phagocytoze polyI:C and deliver them into the endosome. In mouse CD8α⁺ DC direct internalization of polyI:C has remain unproven. Using labeled polyI:C and anti-mouse TLR3 mAb, 11F8,[22] we checked whether the exogenously-added polyI:C encountered with TLR3 in CD8α⁺ DC in vitro. TLR3 (green) was merged with TexasRed-polyI:C 30–120 min after polyI:C stimulation in the culture (**Fig. 6A**). The quantities of CD8α⁺ and CD8α⁻ DC where FITC-polyI:C was incorporated were determined by FACS analysis (**Fig. 6B**). Thus, the process by which polyI:C injected reaches the endosomal TLR3 is delineated in the CD8α⁺ DC.

## Discussion

PolyI:C is an analog of virus dsRNA, and acts as a ligand for TLR3 and RIG-I/MDA5. PolyI:C has been utilized as an adjuvant for enhancement of antitumor immunity for a long time.[29] However, the mechanistic background of the therapeutic potentials of polyI:C against cancer has been poorly illustrated. It induces antitumor NK activation through DC-NK cell-to-cell interaction when CD8α⁺ DC TLR3 is stimulated in the spleen.[11] Besides myeloid cells, however, some tumor cell lines express TLR3 and dsRNA targeting tumor cells may affect the growth rate of tumors,[30] where the receptor-interacting protein (RIP) pathway is involved downstream of TICAM-1.[31] Here we showed evidence that polyI:C injection facilitates maturation of TLR3-positive CD8α⁺ DC (i.e., APC) to trigger CTL induction against exogenous soluble Ags including EG7 lysate or OVA. The TICAM-1 adaptor for TLR3 and IRF-3/7 are involved in the cross-presentation signal in CD8α⁺ DC, but the molecule/mechanism downstream of TICAM-1 that governs cross-presentation remains elusive. Since most of the tumor-associated Ags (TAA) are predicted to be liberated from tumor cells

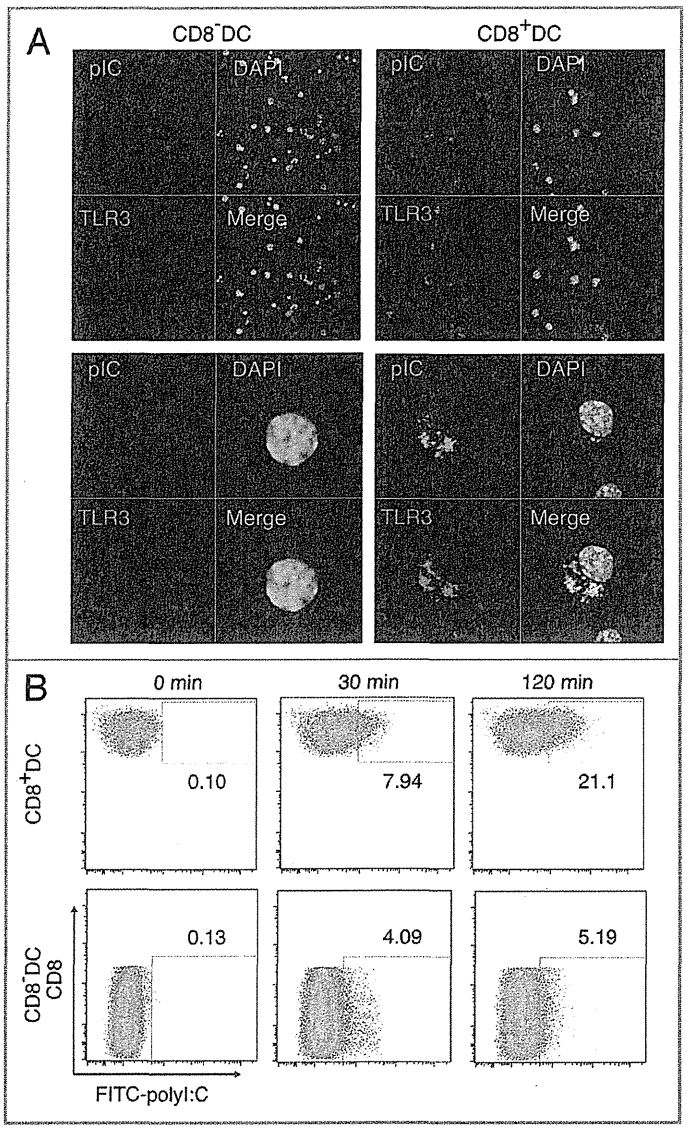


**Figure 6.** PolyI:C encounters TLR3 in CD8α⁺ DC. CD8α⁺ and CD8α⁻ DC were isolated by FACSAriaII and stimulated with 20 μg/ml TexasRed-polyI:C for 2 h. Then cells were stained with Alexa647-antiTLR3 and subjected to confocal microscopic analysis (A). Alternatively, splenic DC isolated by MACS were incubated with FITC-polyI:C for the time shown in figure and analyzed the degrees of polyI:C uptake by FACS (B). Data shown are the representative of three independent experiments.

as soluble Ags, the TICAM-1 pathway in CD8α⁺ DC would be crucial for driving of tumor-specific CTL around the tumor microenvironment. In any route of polyI:C injection, this is true as shown first in this study. Although TICAM-1 is an adaptor of other cytoplasmic sensors, DDX1, DDX21 and DHX36,[32] the antitumor CTL responses are merely relied on TLR3 of CD8α⁺DC in this system. Taken together with previous reports,[11,12] TICAM-1 signaling triggers not only NK activation but also CTL induction.

TLR3 and MDA5 are main sensors for dsRNA and differentially distributed in myeloid cells.[33,34] TLR3 is limitedly expressed in myeloid, epithelial and neuronal cells,[33] whereas MDA5 is ubiquitously expressed including non-myeloid stromal cells.[33] Several reports suggested that i.v. injection of polyI:C predominantly stimulate the stromal cells which express IFNAR,[26] thereby robust type I IFN are liberated from these cells to be a systemic response including cytokinemia and endotoxin-like shock.[35,36] Both TLR3 and MDA5 link to the IRF-3/7-activating kinases leading to the production of IFNα/β.[37,38] Once IFNα/β are released, IFNAR senses it to amplify the Type I IFN production,[39] and reportedly this amplification pathway involves cross-priming of CD8 T cells in viral infection.[18] Tumor progression or metastasis can be suppressed through the IFNAR pathway.[40] These scenarios may be right depending on the conditions employed. Our message is related to what signal pathway is fundamentally required for induction of antitumor CTL in DC. The CTL response is almost completely abrogated in TICAM-1$^{-/-}$ and IRF-3/7$^{-/-}$ mice, but largely remains in IPS-1$^{-/-}$ and IFNAR$^{-/-}$ mice when Ag and polyI:C are extrinsically administered. The results are reproducible in some other tumor-implant models (data not shown), and even in IFNAR$^{-/-}$ mice, TICAM-1-specific genes are upregulated to confer tumor cytotoxicity (**Fig. S6**, Azuma et al., unpublished data). In addition, the upregulation of these genes is independent of IPS-1 knockout in DC. Our results infer that the primary sensing of dsRNA in CD8α⁺ DC is competent to induce cross-presentation, which minimally involves the IPS-1 or IFNAR amplification pathway, at least at a low dose of polyI:C. Yet, subsequent induction of Type I IFN via the IFNAR may further amplify the cross-priming.[18,41] Further studies are needed as to which of the TICAM-1-inducible genes link to the cross-presentation in CD8α⁺ DC.

The main focus of this study was to identify the pathway for transversion of immature DC to the CTL-driving phenotype by co-administration of polyI:C with soluble Ag. The IPS-1 pathway, although barely participates in antitumor CTL driving, can upregulate CD40/CD86 co-stimulators on the membranes of splenic CD8α⁺ and CD8α⁻ DC in response to polyI:C, suggesting that MDA5 does function in the cytoplasm of splenic CD8α⁺ and CD8α⁻ DC to sense polyI:C. However, effective CTL induction happens only in CD8α⁺ DC when stimulated with polyI:C. CD8α⁺ DC express TLR3 but CD8α⁻ DC do not, and CD8α⁺ DC with no TLR3 fail to induce CTL, suggesting that integral co-stimulation by MDA5/IPS-1 is insufficient for DC to induce cross-priming of CD8 T cells: antitumor CTL are not induced until the TICAM-1 signal is provided in DC. At least, sole effect of the IPS-1 pathway and upregulation of co-stimulators on CD8α⁺ DC is limited for cross-priming and induction of antitumor CTL, which result partly reflects those in a previous report where IPS-1 and TICAM-1 harbor a similar potential for CD8 T cell proliferation when

polyI:C (Alum-containing) is employed as an adjuvant for CD8α+ DC to test proliferation of anti-OVA CTL.[21]

A question is why TICAM-1 is dominant to IPS-1 for response to exogenously-added polyI:C in CD8α+ DC. The answer is rooted in the difference of functional behavior between BMDC and CD8α+ DC. TLR3 levels are variable depending upon subsets of DC,[22] which affects DC subset-specific induction of cellular immune response. The high TLR3 expression (partly surface-expressed) is situated in CD8α+ DC before polyI:C stimulation, which is distinct from the properties of F4/80+ Mf and presumably BMDC of low TLR3 expression. The polyI:C-uptake machinery[15] appears to efficiently work in concert with the TLR3/TICAM-1 pathway in CD8α+ DC and this tendency is diminished when CD8α+ DC are pretreated with Alum + polyI:C.[21] Furthermore, there are functional discrepancies between CD8α+ splenic DC and GM-CSF-induced BMDC, which appears to reflect the difference of their TLR3 levels.[22] These results on CD8α+ DC encourage us to develop dsRNA adjuvant immunotherapy supporting TAA soluble vaccines for cancer applicable to humans, which possess the counterpart of CD8α+ DC.

There are two modes of dsRNA-mediated DC maturation, intrinsic and extrinsic modes that are governed by the IPS-1 and TICAM-1 pathways, respectively.[9,34] It is important to elucidate the in vivo qualitative difference in the two pathways in tumor-loading mice. TLR3+ DC/Mf are responsible for CTL driving via an extrinsic route in viral infection.[34] Previous data suggested that dsRNA in infectious cell debris, rather than viral dsRNA produced in the cytoplasm of Ag-presenting cells or autophagosome formation, contribute to fine tuning of DC maturation through extrinsic dsRNA recognition.[16] It is reported that dsRNA-containing debris are generated secondary to infection-mediated cell death,[41] and DC phagocytose by-stander dead cells. Likewise, soluble tumor Ags released from tumor cells usually are extrinsically taken up by APC in patients with cancer.[42] If CTL are successfully induced in therapeutic biotherapy targeted against cancer cells, this extrinsic TICAM-1 pathway must be involved in the therapeutic process.

Cross-presentation occurs in a TAP-dependent[43] and -independent fashions.[44,45] The peptides are transported by TAP into the endoplasmic reticulum (ER) and loaded onto MHC Class I for presentation at the cell surface. ER and phagosome might fuse each other for accelerating cross-presentation.[46] Another possibility is that cross-presentation occurs in early endosomes where TLR3 resides. This early endosome cross-presentation does not always depend on TAP[42-44] but requires TLR stimulation.[34] TLR4/MyD88 pathway is involved in the TAP-dependent early endosome model,[43] where recruitment of TAP to the early endosomes is an essential step for the cross-presentation of soluble Ag. These models together with our genechip analysis of polyI:C-stimulated BMDC suggested that some ER-associated proteins are upregulated in BMDC by polyI:C-TICAM-1 pathway. The results infer that the TLR3/TICAM-1 rather than the TLR4/MyD88 pathway more crucially participates in cross-presentation in response to dsRNA or viral stimuli and facilitates raising CTL antitumor immunity in APC.

Although multiple RNA sensors couple with TICAM-1 and signal to activate the Type I IFN-inducing pathway,[25] at least TLR3 in the CD8α+ DC are critical in CTL driving. CD8α+ DC are a high TLR3 expresser, while BMDC express TLR3 with only low levels.[22] CD8α- DC do not express it.[22] The Ag presentation and TLR3 levels in CD8α+ DC appear reciprocally correlated with the phagocytosing ability of DC. Although the TLR3 mRNA level is downregulated secondary to polyI:C response after maturation, this may not be related to the CD8α+ DC functions. Yet, polyI:C might interact with other cytoplasmic sensors for DC maturation,[32,47]

The route of administration and delivery methods may be important for culminate the polyI:C adjuvant function. The toxic problem has not overcome in the adjuvant therapy using polyI:C[35,36] and this is a critical matter for clinical introduction of dsRNA reagents to immunotherapy. The most problematic is the life-threatening shock induced by polyI:C. Recent advance of polyI:C study suggests that PEI-jet helps efficient uptake of polyI:C into peritoneal macrophages.[48] LC (poly-L-lysine and methylcellulose) has been used as a preservative to reduce the toxic effect of polyI:C.[49] Nanotechnological delivery of polyI:C results in efficient tumor regression.[50] There are many subsets of DC that can be defined by surface markers, and selecting an appropriate administration route can target a specific DC subset. The route for s.c. administration usually mature dermal/epidermal DC or Langerhans cells.[51,52] Some DC subsets with unique properties specialized to CTL induction would work in association with the route of polyI:C administration. Attempting to develop more harmless and efficient dsRNA derivatives will benefit for establishing human adjuvant immunotherapy for cancer.

## Materials and Methods

**Mice.** TICAM-1$^{-/-}$ and IPS-1$^{-/-}$ mice were made in our laboratory and backcrossed more than eight times to adapt C57BL/6 background.[12] IRF-3/7$^{-/-}$ and IFNAR$^{-/-}$ mice were kindly provided by T. Taniguchi (University of Tokyo, Tokyo, Japan). TLR3$^{-/-}$ mice were kindly provided by S. Akira (Osaka University, Osaka, Japan). Rag2$^{-/-}$ and OT-1 mice were kindly provided from Drs N. Ishii (Tohoku University, Sendai, Japan). Rag2$^{-/-}$/OT-1 mice were bred in our laboratory. All mice were maintained under specific pathogen-free conditions in the animal facility of the Hokkaido University Graduate School of Medicine. Animal experiments were performed according to the guidelines set by the animal safety center, Hokkaido University, Japan.

**Cells.** EG7 and C1498 cells were purchased from ATCC and cultured in RPMI1640/10% FCS/55 μM 2-ME/1 mM sodium pyruvate and RPMI1640/10% FCS/25 ng/ml 2-ME, respectively. Mouse splenocytes, OT-1 T cell, CD8α+ DC and CD8α- DC were harvested from the spleen and cultured in RPMI1640/10% FCS/55 μM 2-ME/10 mM HEPES.[41] B16D8 cells were cultured in RPMI/10% FCS as described previously.[12]

**Reagents and antibodies.** Ovalbumin (OVA) and polyI:C (polyI:C) were purchased from SIGMA and Amersham Biosciences, respectively. $OVA_{257-264}$ peptide (SIINFEKL: SL8)

and OVA ($H2K^b$-SL8) Tetramer were from MBL. Following Abs were purchased: anti-CD3ε (145-2C11), anti-CD8β (53-6.7), anti-CD11c (N418), anti-CD16/32 (93), anti-CD69 (H1.2F3) and anti-IFNγ(XMG1.2) Abs from BioLegend, anti-B220 (RA3-6B2), anti-CD4 (L3T4), anti-CD40 (1C10), anti-CD86 (GL1), and anti-MHC I-SL8 (25-D1.16) Abs from eBiosciences, anti-TCR-Vβ5.1/5.2 Ab and ViaProbe from BD Biosciences. The Rat anti-mouse TLR3 mAb (11F8) was kindly provided by David M. Segal (National Institute of Health, Bethesda, MD). To rule out LPS contamination, we treated OVA or other reagents with 200 μg/ml of Polymixin B for 30 min at 37°C before use. Texas Red- or FITC-labeled poly(I:C) was prepared using the 5' EndTag™ Nucleic Acid Labeling System (Vector Laboratories) according to the manufacturers instructions.

**Tumor challenge and poly I:C therapy.** Mice were shaved at the back and s.c. injected with 200 μl of $2 \times 10^6$ syngenic EG7 cells in PBS. Tumor volumes were measured at regular intervals by using a caliper. Tumor volume was calculated by using the formula: Tumor volume ($cm^3$) = (long diameter) × (short diameter)$^2$ × 0.4. A volume of 50 μl of a mixture consisting of the lysate of $2 \times 10^5$ EG7 cells with or without 50 μg of poly I:C (polyI:C) was s.c. injected around the tumor. We added no other emulsified reagent for immunization since we want to role out the conditional effect of the Ag/polyI:C. The treatments were started when the average of tumor volumes reached at 0.4–0.8 $cm^3$ and performed twice per week. EG7 lysate were prepared by three times freeze/thaw cycles (-140°C/37°C) in PBS, with removal of cell debris by centrifugation at 6,000 g for 10 min.[53] To deplete CD8 T cells, mice were i.p. injected with hybridoma ascites of anti-CD8β mAb. The dose of antibody and the treatment regimens were determined in preliminary studies by using the same lots of antibody used for the experiments. Depletion of the desired cell populations by this treatment was confirmed by FACS for the entire duration of the study.

**Evaluation of T cell activity in tumor-bearing mice.** Draining inguinal LN cells were harvested from tumor-bearing mice after 24 h from the last polyI:C treatment. The activity of T cells was evaluated by CD69 expression and IL-2/IFNγ production. These cells were stained with FITC-CD8α, PE-CD69, PerCP/Cy5.5-7AAD and APC-CD3ε. To check cytokine production, LN cells were cultured for 3 d in vitro in the presence or absence of EG7 lysates and IL-2 and IFNγ productions were determined by Cytokine Beads Array (CBA) assay (BD). To assess the cytotoxic activity of CTL, standard $^{51}Cr$ release assay was performed. For CTL expansion, $2.5 \times 10^6$ LN cells were co-cultured with $1.25 \times 10^5$ mitomycin C-treated EG7 cells in the presence of 10 U/ml IL-2 for 5 d. Then, LN cells were incubated with $^{51}Cr$-labeled EG7 or C1498 cells for 4 h and determined cytotoxic activity. The cell-specific cytotoxicity was calculated with subtracting the cytotoxity for C1498 from for EG7 cells.

**Antigen-specific T cell expansion in vivo.** Mice were i.p. immunized with 1 mg of OVA and 150 μg of poly I:C. After 7 d, spleens were homogenized and stained with FITC-CD8α and PE-OVA Tetramer for detecting OVA-specific CD8 T cell populations. For intracellular cytokine detection, splenocytes were cultured with or without 100 nM OVA peptide (SIINFEKL; SL8) for 8 h and 10 μg/ml of Brefeldin A (Sigma-Aldrich) was added to the culture in the last 4 h. Then cells were stained with PE-anti-CD8α and fixed/permeabilized with Cytofix/Cytoperm (BD Biosciences) according to manufacturer's instruction. Then, fixed/permeabilized cells were further stained with APC-anti-IFNγ. Stained cells were analyzed with FACSCalibur (BD Biosciences) and FlowJo software (Tree Star).

**In vivo CTL assay.** The in vivo CTL assay was performed as described.[54] In brief, WT, TICAM-$1^{-/-}$, MAVS$^{-/-}$ and IRF-$3/7^{-/-}$ mice were i.v. administered with PBS, 10 μg of OVA or OVA with 50 μg of polyI:C. After 5 d, $2 \times 10^7$ target cells (see below) were i.v. injected to other irrelevant mice and 8 h later, the OVA-specific cytotoxicity was measured by FACSCalibur. Target cells were 1:1 mixture of 2 μM SL8-pulsed, 5 μM CFSE-labeled splenocytes and SL8-unpulesed, 0.5 μM CFSE-labeled splenocytes. OVA-specific cytotoxicity was calculated with a formula: {1-(Primed [$CFSE^{high}$(%)/$CFSE^{low}$(%)]/Unprimed [$CFSE^{high}$(%)/$CFSE^{low}$(%)]} × 100.

**DC preparation.** DCs were prepared from spleens of mice, as described previously.[55] In brief, collagenase-digested spleen cells were treated with ACK buffer and then washed with PBS twice. Then splenocytes were positively isolated with anti-CD11c MicroBeads. $CD11c^+$ cells were acquired routinely about ≥ 80% purity. Further, to highly purify $CD8\alpha^+$ and $CD8\alpha^-$ DCs, spleen DC were stained with FITC-CD8α, PE-B220, PE/Cy7-CD11c and PerCP5.5-7AAD. $CD8\alpha^+$ or $CD8\alpha^-$ $CD11c^+B220^-$ DCs were purified on FACSAriaII (BD). The purity of the cells was ≥ 98%.

**OT-1 proliferation assay.** Ten micrograms of OVA with or without 50 μg of polyI:C were i.v. injected to WT, TICAM-$1^{-/-}$, IPS-$1^{-/-}$ and DKO mice. After 4 h, $CD8\alpha^+$ or $CD8\alpha^-$ DC were purified from the spleen. $2.5 \times 10^4$ $CD8\alpha^+$ or $CD8\alpha^-$ DC were co-cultured with $5 \times 10^4$ 1 μM CFSE-labeled Rag$2^{-/-}$/OT-1 T cells for 3 d in 96-well round bottom plate. These cells were stained with PE-anti-TCR-Vβ5.1,5.2 and APC-anti-CD3ε and T cell proliferation was analyzed by CFSE dilution using FACSCalibur. Additionally, IFNγ in the culture supernatant was measured by CBA assay.

**Statistical analysis.** P-values were calculated with one-way analysis of variance (ANOVA) with Bonferroni's test. Error bars represent the SD or SEM between samples.

### Disclosure of Potenial Conflicts of Interest

No potential conflicts of interest were disclosed.


### Acknowledgment

We are grateful to Drs. T. Taniguchi (University Tokyo, Tokyo), N. Ishii (Tohoku University, Sendai) and D.M. Segel (NCI, Bethesda) for providing us with IRF-$3/7^{-/-}$ mice, OT-1 mice and anti-monse TLR3 mAb, respectively. Invaluable discussions about the peptide vaccine therapy with Dr. N. Satoh (Sapporo Medical

University, Sapporo) are gratefully acknowledged. We thank Drs H. Takaki, J. Kasamatsu, H.H. Aly, and H. Shime in our lab for their critical comments on this study.

This work was supported in part by Grants-in-Aid from the Ministry of Education, Science, and Culture (Specified Project for Advanced Research, MEXT) and the Ministry of Health, Labor, and Welfare of Japan, and by the Takeda and the Waxmann Foundations. Financial supports by a MEXT Grant-in-Project "The Carcinogenic Spiral" is gratefully acknowledged.

### Supplemental Materials

Supplemental materials may be found here:
http://www.landesbioscience.com/journals/oncoimmunology/article/19893/

### References

1. Iwasaki A, Medzhitov R. Regulation of adaptive immunity by the innate immune system. Science 2010; 327:291-5; PMID:20075244; http://dx.doi.org/10.1126/science.1183021
2. Seya T, Shime H, Ebihara T, Oshiumi H, Matsumoto M. Pattern recognition receptors of innate immunity and their application to tumor immunotherapy. Cancer Sci 2010; 101:313-20; PMID:20059475; http://dx.doi.org/10.1111/j.1349-7006.2009.01442.x
3. Akira S. Toll-like receptor signaling. J Biol Chem 2003; 278:38105-8; PMID:12893815; http://dx.doi.org/10.1074/jbc.R300028200
4. Kawai T, Akira S. The roles of TLRs, RLRs and NLRs in pathogen recognition. Int Immunol 2009; 21:317-37; PMID:19246554; http://dx.doi.org/10.1093/intimm/dxp017
5. Longman RS, Braun D, Pellegrini S, Rice CM, Darnell RB, Albert ML. Dendritic-cell maturation alters intracellular signaling networks, enabling differential effects of IFN-alpha/beta on antigen cross-presentation. Blood 2007; 109:1113-22; PMID:17018853; http://dx.doi.org/10.1182/blood-2006-05-023465
6. Shinohara ML, Kim JH, Garcia VA, Cantor H. Engagement of the type I interferon receptor on dendritic cells inhibits T helper 17 cell development: role of intracellular osteopontin. Immunity 2008; 29:68-78; PMID:18619869; http://dx.doi.org/10.1016/j.immuni.2008.05.008
7. Diebold SS. Recognition of viral single-stranded RNA by Toll-like receptors. Adv Drug Deliv Rev 2008; 60:813-23; PMID:18241955; http://dx.doi.org/10.1016/j.addr.2007.11.004
8. Matsumoto M, Oshiumi H, Seya T. Antiviral responses induced by the TLR3 pathway. Rev Med Virol 2011. Epub ahead of print. PMID:21312311; http://dx.doi.org/10.1002/rmv.680
9. Yoneyama M, Fujita T. RIG-I family RNA helicases: cytoplasmic sensor for antiviral innate immunity. Cytokine Growth Factor Rev 2007; 18:545-51; PMID:17683970; http://dx.doi.org/10.1016/j.cytogfr.2007.06.023
10. Seya T, Matsumoto M. The extrinsic RNA-sensing pathway for adjuvant immunotherapy of cancer. Cancer Immunol Immunother 2009; 58:1175-84; PMID:19184005; http://dx.doi.org/10.1007/s00262-008-0652-9
11. Akazawa T, Ebihara T, Okuno M, Okuda Y, Shingai M, Tsujimura K, et al. Antitumor NK activation induced by the Toll-like receptor 3-TICAM-1 (TRIF) pathway in myeloid dendritic cells. Proc Natl Acad Sci U S A 2007; 104:252-7; PMID:17190817; http://dx.doi.org/10.1073/pnas.0605978104
12. Ebihara T, Azuma M, Oshiumi H, Kasamatsu J, Iwabuchi K, Matsumoto K, et al. Identification of a polyI:C-inducible membrane protein that participates in dendritic cell-mediated natural killer cell activation. J Exp Med 2010; 207:2675-87; PMID:21059856; http://dx.doi.org/10.1084/jem.20091573
13. Perrot I, Deauvieau F, Massacrier C, Hughes N, Garrone P, Durand I, et al. TLR3 and Rig-like receptor on myeloid dendritic cells and Rig-like receptor on human NK cells are both mandatory for production of IFN-gamma in response to double-stranded RNA. J Immunol 2010; 185:2080-8; PMID:20639488; http://dx.doi.org/10.4049/jimmunol.1000532
14. Bevan MJ. Cross-priming for a secondary cytotoxic response to minor H antigens with H-2 congenic cells which do not cross-react in the cytotoxic assay. J Exp Med 1976; 143:1283-8; PMID:1083422; http://dx.doi.org/10.1084/jem.143.5.1283
15. Datta SK, Redecke V, Prilliman KR, Takabayashi K, Corr M, Tallant T, et al. A subset of Toll-like receptor ligands induces cross-presentation by bone marrow-derived dendritic cells. J Immunol 2003; 170:4102-10; PMID:12682240
16. Schulz O, Diebold SS, Chen M, Näslund TI, Nolte MA, Alexopoulou L, et al. Toll-like receptor 3 promotes cross-priming to virus-infected cells. Nature 2005; 433:887-92; PMID:15711573; http://dx.doi.org/10.1038/nature03326
17. Kono H, Rock KL. How dying cells alert the immune system to danger. Nat Rev Immunol 2008; 8:279-89; PMID:18340345; http://dx.doi.org/10.1038/nri2215
18. Le Bon A, Etchart N, Rossmann C, Ashton M, Hou S, Gewert D, et al. Cross-priming of CD8+ T cells stimulated by virus-induced type I interferon. Nat Immunol 2003; 4:1009-15; PMID:14502286; http://dx.doi.org/10.1038/ni978
19. Bennett SR, Carbone FR, Karamalis F, Miller JF, Heath WR. Induction of a CD8+ cytotoxic T lymphocyte response by cross-priming requires cognate CD4+ T cell help. J Exp Med 1997; 186:65-70; PMID:9206998; http://dx.doi.org/10.1084/jem.186.1.65
20. Shimizu K, Kurosawa Y, Taniguchi M, Steinman RM, Fujii S. Cross-presentation of glycolipid from tumor cells loaded with alpha-galactosylceramide leads to potent and long-lived T cell mediated immunity via dendritic cells. J Exp Med 2007; 204:2641-53; PMID:17923500; http://dx.doi.org/10.1084/jem.20070458
21. Kumar H, Koyama S, Ishii KJ, Kawai T, Akira S. Cutting edge: cooperation of IPS-1- and TRIF-dependent pathways in poly IC-enhanced antibody production and cytotoxic T cell responses. J Immunol 2008; 180:683-7; PMID:18178804
22. Jelinek I, Leonard JN, Price GE, Brown KN, Meyer-Manlapat A, Goldsmith PK, et al. TLR3-specific double-stranded RNA oligonucleotide adjuvants induce dendritic cell cross-presentation, CTL responses, and antiviral protection. J Immunol 2011; 186:2422-9; PMID:21242525; http://dx.doi.org/10.4049/jimmunol.1002845
23. Wang Y, Cella M, Gilfillan S, Colonna M. Cutting edge: polyinosinic:polycytidylic acid boosts the generation of memory CD8 T cells through melanoma differentiation-associated protein 5 expressed in stromal cells. J Immunol 2010; 184:2751-5; PMID:20164430; http://dx.doi.org/10.4049/jimmunol.0903201
24. Carbone FR, Bevan MJ. Induction of ovalbumin-specific cytotoxic T cells by in vivo peptide immunization. J Exp Med 1989; 169:603-12; PMID:2784478; http://dx.doi.org/10.1084/jem.169.3.603
25. Asano J, Tada H, Onai N, Sato T, Horie Y, Fujimoto Y, et al. Nucleotide oligomerization binding domain-like receptor signaling enhances dendritic cell-mediated cross-priming in vivo. J Immunol 2010; 184:736-45; PMID:20008287; http://dx.doi.org/10.4049/jimmunol.0900726
26. McCartney S, Vermi W, Gilfillan S, Cella M, Murphy TL, Schreiber RD, et al. Distinct and complementary functions of MDA5 and TLR3 in poly(I:C)-mediated activation of mouse NK cells. J Exp Med 2009; 206:2967-76; PMID:19995959; http://dx.doi.org/10.1084/jem.20091181
27. Watanabe A, Taremaru M, Saeki K, Shibata S, Shime H, Yoshimura A, et al. Raftlin is involved in the nucleocapture complex to induce poly(I:C)-mediated TLR3 activation. J Biol Chem 2011; 286:10702-11; PMID:21266579; http://dx.doi.org/10.1074/jbc.M110.185793
28. Itoh K, Watanabe A, Funami K, Seya T, Matsumoto M. The clathrin-mediated endocytic pathway participates in dsRNA-induced IFN-beta production. J Immunol 2008; 181:5522-9; PMID:18832709
29. Talmadge JE, Adams J, Phillips H, Collins M, Lenz B, Schneider M, et al. Immunomodulatory effects in mice of polyinosinic-polycytidylic acid complexed with poly-L-lysine and carboxymethylcellulose. Cancer Res 1985; 45:1058-65; PMID:3155990
30. Conforti R, Ma Y, Morel Y, Paturel C, Terme M, Viaud S, et al. Opposing effects of toll-like receptor (TLR3) signaling in tumors can be therapeutically uncoupled to optimize the anticancer efficacy of TLR3 ligands. Cancer Res 2010; 70:490-500; PMID:20068181; http://dx.doi.org/10.1158/0008-5472.CAN-09-1890
31. Kaiser WJ, Offermann MK. Apoptosis induced by the toll-like receptor adaptor TRIF is dependent on its receptor interacting protein homotypic interaction motif. J Immunol 2005; 174:4942-52; PMID:15814722
32. Zhang Z, Kim T, Bao M, Facchinetti V, Jung SY, Ghaffari AA, et al. DDX1, DDX21, and DHX36 helicases form a complex with the adaptor molecule TRIF to sense dsRNA in dendritic cells. Immunity 2011; 34:866-78; PMID:21703541; http://dx.doi.org/10.1016/j.immuni.2011.03.027
33. Gitlin L, Barchet W, Gilfillan S, Cella M, Beutler B, Flavell RA, et al. Essential role of mda-5 in type I IFN responses to polyriboinosinic:polyribocytidylic acid and encephalomyocarditis picornavirus. Proc Natl Acad Sci U S A 2006; 103:8459-64; PMID:16714379; http://dx.doi.org/10.1073/pnas.0603082103
34. Matsumoto M, Seya T. TLR3: interferon induction by double-stranded RNA including poly(I:C). Adv Drug Deliv Rev 2008; 60:805-12; PMID:18262679; http://dx.doi.org/10.1016/j.addr.2007.11.005

35. Absher M, Stinebring WR. Toxic properties of a synthetic double-stranded RNA. Endotoxin-like properties of poly I. poly C, an interferon stimulator. Nature 1969; 223:715-7; PMID:5805520; http://dx.doi.org/10.1038/223715a0
36. Berry LJ, Smythe DS, Colwell LS, Schoengold RJ, Actor P. Comparison of the effects of a synthetic polyribonucleotide with the effects of endotoxin on selected host responses. Infect Immun 1971; 3:444-8; PMID:16557994
37. Sasai M, Shingai M, Funami K, Yoneyama M, Fujita T, Matsumoto M, et al. NAK-associated protein 1 participates in both the TLR3 and the cytoplasmic pathways in type I IFN induction. J Immunol 2006; 177:8676-83; PMID:17142768
38. Ishikawa H, Barber GN. STING is an endoplasmic reticulum adaptor that facilitates innate immune signalling. Nature 2008; 455:674-8; PMID:18724357; http://dx.doi.org/10.1038/nature07317
39. Taniguchi T, Takaoka A. A weak signal for strong responses: interferon-alpha/beta revisited. Nat Rev Mol Cell Biol 2001; 2:378-86; PMID:11331912; http://dx.doi.org/10.1038/35073080
40. Ogasawara S, Yano H, Momosaki S, Akiba J, Nishida N, Kojiro S, et al. Growth inhibitory effects of IFN-beta on human liver cancer cells in vitro and in vivo. J Interferon Cytokine Res 2007; 27:507-16; PMID:17572015; http://dx.doi.org/10.1089/jir.2007.0183
41. Ebihara T, Shingai M, Matsumoto M, Wakita T, Seya T. Hepatitis C virus-infected hepatocytes extrinsically modulate dendritic cell maturation to activate T cells and natural killer cells. Hepatology 2008; 48:48-58; PMID:18537195; http://dx.doi.org/10.1002/hep.22337
42. Chaput N, Conforti R, Viaud S, Spatz A, Zitvogel L. The Janus face of dendritic cells in cancer. Oncogene 2008; 27:5920-31; PMID:18836473; http://dx.doi.org/10.1038/onc.2008.270
43. Burgdorf S, Schölz C, Kautz A, Tampé R, Kurts C. Spatial and mechanistic separation of cross-presentation and endogenous antigen presentation. Nat Immunol 2008; 9:558-66; PMID:18376402; http://dx.doi.org/10.1038/ni.1601
44. Shen L, Sigal LJ, Boes M, Rock KL. Important role of cathepsin S in generating peptides for TAP-independent MHC class I crosspresentation in vivo. Immunity 2004; 21:155-65; PMID:15308097; http://dx.doi.org/10.1016/j.immuni.2004.07.004
45. Kurotaki T, Tamura Y, Ueda G, Oura J, Kutomi G, Hirohashi Y, et al. Efficient cross-presentation by heat shock protein 90-peptide complex-loaded dendritic cells via an endosomal pathway. J Immunol 2007; 179:1803-13; PMID:17641047
46. Gagnon E, Duclos S, Rondeau C, Chevet E, Cameron PH, Steele-Mortimer O, et al. Endoplasmic reticulum-mediated phagocytosis is a mechanism of entry into macrophages. Cell 2002; 110:119-31; PMID:12151002; http://dx.doi.org/10.1016/S0092-8674(02)00797-3
47. Samuel CE. Antiviral actions of interferons. Clin Microbiol Rev 2001; 14:778-809; PMID:11585785; http://dx.doi.org/10.1128/CMR.14.4.778-809.2001
48. Wu CY, Yang HY, Monie A, Ma B, Tsai HH, Wu TC, et al. Intraperitoneal administration of poly(I:C) with polyethylenimine leads to significant antitumor immunity against murine ovarian tumors. Cancer Immunol Immunother 2011; 60:1085-96; PMID:21526359; http://dx.doi.org/10.1007/s00262-011-1013-7
49. Longhi MP, Trumpfheller C, Idoyaga J, Caskey M, Matos I, Kluger C, et al. Dendritic cells require a systemic type I interferon response to mature and induce CD4+ Th1 immunity with poly IC as adjuvant. J Exp Med 2009; 206:1589-602; PMID:19564349; http://dx.doi.org/10.1084/jem.20090247
50. Kitano S, Kageyama S, Nagata Y, Miyahara Y, Hiasa A, Naota H, et al. HER2-specific T-cell immune responses in patients vaccinated with truncated HER2 protein complexed with nanogels of cholesteryl pullulan. Clin Cancer Res 2006; 12:7397-405; PMID:17189412; http://dx.doi.org/10.1158/1078-0432.CCR-06-1546
51. Kushwah R, Hu J. Complexity of dendritic cell subsets and their function in the host immune system. Immunology 2011; 133:409-19; PMID:21627652; http://dx.doi.org/10.1111/j.1365-2567.2011.03457.x
52. Asano K, Nabeyama A, Miyake Y, Qiu CH, Kurita A, Tomura M, et al. CD169-positive macrophages dominate antitumor immunity by crosspresenting dead cell-associated antigens. Immunity 2011; 34:85-95; PMID:21194983; http://dx.doi.org/10.1016/j.immuni.2010.12.011
53. Galea-Lauri J, Wells JW, Darling D, Harrison P, Farzaneh F. Strategies for antigen choice and priming of dendritic cells influence the polarization and efficacy of antitumor T-cell responses in dendritic cell-based cancer vaccination. Cancer Immunol Immunother 2004; 53:963-77; PMID:15146294; http://dx.doi.org/10.1007/s00262-004-0542-8
54. Durand V, Wong SY, Tough DF, Le Bon A. Shaping of adaptive immune responses to soluble proteins by TLR agonists: a role for IFN-α/β. Immunol Cell Biol 2004; 82:596-602; PMID:15550117; http://dx.doi.org/10.1111/j.0818-9641.2004.01285.x
55. Yamazaki S, Okada K, Maruyama A, Matsumoto M, Yagita H, Seya T. TLR2-dependent induction of IL-10 and Foxp3+ CD25+ CD4+ regulatory T cells prevents effective anti-tumor immunity induced by Pam2 lipopeptides in vivo. PLoS One 2011; 6:e18833; PMID:21533081; http://dx.doi.org/10.1371/journal.pone.0018833

# Toll-like receptor 3 signaling converts tumor-supporting myeloid cells to tumoricidal effectors

Hiroaki Shime[a], Misako Matsumoto[a], Hiroyuki Oshiumi[a], Shinya Tanaka[b], Akio Nakane[c], Yoichiro Iwakura[d], Hideaki Tahara[e], Norimitsu Inoue[f], and Tsukasa Seya[a,1]

[a]Department of Microbiology and Immunology, and [b]Department of Cancer Pathology, Graduate School of Medicine, Hokkaido University, Kita-ku, Sapporo 060-8638, Japan; [c]Department of Microbiology and Immunology, Graduate School of Medicine, Hirosaki University, Zaifu-cho, Hirosaki 036-8562, Japan; [d]Laboratory of Molecular Pathogenesis, Center for Experimental Medicine and Systems Biology, and [e]Department of Surgery and Bioengineering, Advanced Clinical Research Center, Institute of Medical Science, University of Tokyo, Shirokanedai, Minato-ku, Tokyo 108-8639, Japan; and [f]Department of Molecular Genetics, Osaka Medical Center for Cancer, Nakamichi, Higashinari-ku, Osaka 537-8511, Japan

Edited by Ruslan Medzhitov, Yale University School of Medicine, New Haven, CT, and approved December 20, 2011 (received for review August 11, 2011)

**Smoldering inflammation often increases the risk of progression for malignant tumors and simultaneously matures myeloid dendritic cells (mDCs) for cell-mediated immunity. PolyI:C, a dsRNA analog, is reported to induce inflammation and potent antitumor immune responses via the Toll-like receptor 3/Toll–IL-1 receptor domain-containing adaptor molecule 1 (TICAM-1) and melanoma differentiation-associated protein 5/IFN-β promoter stimulator 1 (IPS-1) pathways in mDCs to drive activation of natural killer cells and cytotoxic T lymphocytes. Here, we found that i.p. or s.c. injection of polyI:C to Lewis lung carcinoma tumor-implant mice resulted in tumor regression by converting tumor-supporting macrophages (Mfs) to tumor suppressors. F4/80$^{+}$/Gr1$^{-}$ Mfs infiltrating the tumor respond to polyI:C to rapidly produce inflammatory cytokines and thereafter accelerate M1 polarization. TNF-α was increased within 1 h in both tumor and serum upon polyI:C injection into tumor-bearing mice, followed by tumor hemorrhagic necrosis and growth suppression. These tumor responses were abolished in TNF-α$^{-/-}$ mice. Furthermore, F4/80$^{+}$ Mfs in tumors extracted from polyI:C-injected mice sustained Lewis lung carcinoma cytotoxic activity, and this activity was partly abrogated by anti–TNF-α Ab. Genes for supporting M1 polarization were subsequently up-regulated in the tumor-infiltrating Mfs. These responses were completely abrogated in TICAM-1$^{-/-}$ mice, and unaffected in myeloid differentiation factor 88$^{-/-}$ and IPS-1$^{-/-}$ mice. Thus, the TICAM-1 pathway is not only important to mature mDCs for cross-priming and natural killer cell activation in the induction of tumor immunity, but also critically engaged in tumor suppression by converting tumor-supporting Mfs to those with tumoricidal properties.**

Toll-like receptor | tumor-associated macrophages | TRIF

Inflammation followed by bacterial and viral infections triggers a high risk of cancer and promotes tumor development and progression (1, 2). Long-term use of anti-inflammatory drugs has been shown to reduce—if not eliminate—the risk of cancer, as demonstrated by a clinical study of aspirin and colorectal cancer occurrence (3). Inflammatory cytokines facilitate tumor progression and metastasis in most cases. Innate immune response and the following cellular events are closely concerned with the formation of the tumor microenvironment (4, 5).

By contrast, inflammation induced by microbial preparations was applied to patients with cancer for therapeutic potential as Coley vaccine with some success. A viral replication product, dsRNA and its analog polyI:C (6, 7), induced acute inflammation, and has been expected to be a promising therapeutic agent against cancer. Although polyI:C exerts life-threatening cytokinemia (8), trials for its clinical use as an adjuvant continued because of its high therapeutic potential (9, 10). Pathogen-associated molecular patterns (PAMPs) and host cell factors induced secondary to PAMP–host cell interaction act as a double-edged sword in cancer prognosis and require understanding their multifarious functional properties in the tumor environment.

Recent advances in the study of innate immunity show how polyI:C suppresses tumor progression (11). PolyI:C is a synthetic compound that serves as an agonist for pattern-recognition receptors (PRRs), Toll-like receptor 3 (TLR3), and melanoma differentiation-associated protein 5 (MDA5) (12–14). Although TLR3 and MDA5 signals are characterized as myeloid differentiation factor 88 (MyD88) independent (15, 16), they have immune effector-inducing properties (12–14, 17). TLR3 couples with the Toll–IL-1 receptor domain-containing adaptor molecule 1 (TICAM-1, also known as TRIF), and MDA5 couples with the IFN-β promoter stimulator 1 (IPS-1, also known as Cardif, MAVS, or VISA) (11, 15). Possible functions for the TICAM-1 and IPS-1 signaling pathways have been investigated by using gene-disrupted mice (15); although they activate the same downstream transcription factors NF-κB and IFN regulatory factor 3 (IRF-3) (15, 18), they appear to distinctly modulate myeloid dendritic cells (mDCs) and macrophages (Mfs) to drive effector lymphocytes (19, 20).

Tumor microenvironments frequently involve myeloid-derived suppressor cells (MDSCs), tumor-associated macrophages (TAMs), and immature mDCs (1, 21). These myeloid cells express PRR through which they are functionally activated. Once the inflammation process is triggered, immature mDCs turn mature so that they are capable of antigen cross-presentation and able to activate immune effector cells, which would act to protect the host system and damage the undesirable tumor cells (22). However, TAMs and MDSCs play a major role in establishing a favorable environment for tumor cell development by suppressing antitumor immunity and recruiting host immune cells to support tumor cell survival, motility, and invasion (23–25). Although these myeloid cell scenarios have been studied with interest, how the PRR signal in these myeloid cells links regulation of tumor progression has yet to be elucidated.

Here we show that TICAM-1 but not IPS-1 signal in tumor-infiltrating Mfs is engaged in conversion of the TAM-like Mfs to tumoricidal effectors. We investigated the molecular mechanisms in Mfs underlying the phenotype switch from tumor supporting to tumor suppressing by treating cells with polyI:C and found that the TICAM-1–inducing TNF-α and M1 polarization are crucial for eliciting tumoricidal activity in TAMs.

## Results

**In Vivo Effect of PolyI:C on Implant Lewis Lung Carcinoma Tumor.** I.p. injection of polyI:C rapidly induced hemorrhagic necrosis in 3LL tumors implanted in WT mice, which was established >12 h after polyI:C treatment (Fig. 1*A*). The polyI:C-dependent hemorrhagic necrosis did not occur in TNF-α$^{-/-}$ mice (Fig. 1*A*). Histological

Author contributions: H.S., M.M., and T.S. designed research; H.S., H.O., and S.T. performed research; H.O., A.N., Y.I., and H.T. contributed new reagents/analytic tools; M.M. and N.I. analyzed data; and H.S. and T.S. wrote the paper.

The authors declare no conflict of interest.

This article is a PNAS Direct Submission.

[1]To whom correspondence should be addressed. E-mail: seya-tu@pop.med.hokudai.ac.jp.

This article contains supporting information online at www.pnas.org/lookup/suppl/doi:10.1073/pnas.1113099109/-/DCSupplemental.

and immunohistochemical analysis revealed vascular damage in the necrotic lesion, where disruption of vascular endothelial cells was indicated by fragmented $CD31^+$ marker (Fig. S1). Although the polyI:C signal is delivered by TICAM-1 and IPS-1 adaptors (11, 13), the hemorrhagic necrosis was largely alleviated in TICAM-$1^{-/-}$ mice but not in IPS-$1^{-/-}$ mice (Fig. 1*A*). The results suggest that polyI:C is a reagent that induces Lewis lung carcinoma (3LL) hemorrhagic necrosis, and the TICAM-1 pathway and its products, including TNF-α, are preferentially involved in this response.

3LL implant tumors grew well in WT C57BL6 mice. PolyI:C, when i.p. injected, resulted in tumor growth retardation (Fig. 1*B*). The retardation of tumor growth by polyI:C was also impaired in TNF-$\alpha^{-/-}$ mice (Fig. 1*B*), suggesting that TNF-α is a critical effector for not only induction of hemorrhagic necrosis but also further 3LL tumor regression. To investigate the signaling pathway involved in the tumor growth retardation by polyI:C, we challenged WT, MyD88$^{-/-}$, TICAM-$1^{-/-}$, and IPS-$1^{-/-}$ mice with 3LL implantation and then treated the mice with i.p. injection of polyI:C. 3LL growth retardation was observed in both IPS-$1^{-/-}$ (Fig. 1*C*) and MyD88$^{-/-}$ mice, to a similar extent to WT mice. In contrast, polyI:C-dependent tumor growth retardation was abrogated in TICAM-$1^{-/-}$ mice (Fig. 1*D*). The size differences of the implanted tumors became significant within 2 d after polyI:C treatment, suggesting that the molecular effector for tumor regression is induced early and its upstream is TICAM-1. Similar results were obtained with MC38 implant tumor (Fig. S2*A*), which is TNF-α sensitive and MHC class I positive (Table S1) (26).

PolyI:C is a reagent that induces natural killer (NK) cell activation in MHC class I-negative tumors (12), and 3LL cells are class I negative and NK cell sensitive (Table S1) (27, 28). We tested whether NK cells activated by polyI:C damage the 3LL tumor in mice. Tumor growth was not affected by pretreatment of the mice with anti-NK1.1 Ab in this model (Fig. S3). Thus, NK cells, at least the $NK1.1^+$ cells, have a negligible ability to retard tumor growth in vivo.

**PolyI:C Induces TNF-α Through the TICAM-1 Pathway in Mice.** To test whether polyI:C treatment had elicited TNF-α production in vivo, we investigated the cytokine profiles of serum from polyI:C-stimulated WT and IPS-$1^{-/-}$ and TICAM-$1^{-/-}$ mice by ELISA. Prominent differences in TNF-α levels were observed in serum collected from polyI:C-injected WT and TICAM-$1^{-/-}$ mice. Serum TNF-α levels in WT and IPS-$1^{-/-}$ mice were significantly higher than that in TICAM-$1^{-/-}$ mice within 1 h after polyI:C injection (Fig. S4 *A* and *B*). IFN-β is a main output for polyI:C stimulation (11), and its production was decreased in TICAM-$1^{-/-}$ mice and totally abrogated in IPS-$1^{-/-}$ mice (Fig. S4*C*). Taken together, the data indicate that the TICAM-1 pathway was able to sustain a high TNF-α level in the early phase of polyI:C treatment, which is independent of IPS-1 and subsequent production of IFN-β.

**TICAM-$1^+$ Cells in Tumor Produces TNF-α in Response to PolyI:C Stimulation.** Using the 3LL implant WT, IPS-$1^{-/-}$, and TICAM-$1^{-/-}$ mouse models, we tested whether polyI:C-induced early TNF-α was responsible for the lately observed tumor regression. Time-course analyses of the polyI:C-induced TNF-α protein levels were performed by ELISA using serum samples and tumors extracted from the experimental mice. The tumor TNF-α levels in WT and IPS-$1^{-/-}$ mice increased at 2 h after polyI:C i.p. injection (Fig. 2*A*). The serum TNF-α levels in both were rapidly up-regulated within 1 h after polyI:C injection, although in WT the levels continued to increase but in IPS-$1^{-/-}$ mice gradually decreased (Fig. 2*B*). In TICAM-$1^{-/-}$ mice, however, no appreciable up-regulation of TNF-α protein was detected in either tumor or serum samples during the early time-course tested. To test whether the induced TNF-α protein was generated de novo in tumors, we examined the corresponding mRNA levels in excised tumors (Fig. 2*C* and Table S2). The TNF-α mRNA levels peaked between 1 and 2 h after polyI:C injection, whereas the TNF-α protein level was kept high at >2 h after polyI:C injection in tumor as well as serum. In the TICAM-$1^{-/-}$ mice, TNF-α production was largely abrogated in the tumor and serum samples, suggesting that TNF-α was mainly produced and secreted in response to polyI:C stimulation from the TLR3/TICAM-$1^+$ cells within the tumor.

**F4/80$^+$/Gr-$1^-$ Mfs in 3LL Tumor Produce TNF-α Leading to Tumor Damage.** We next investigated the cell types that had infiltrated the tumor by using various Mf markers in FACS analysis and tumor samples extracted at 1 h after polyI:C injection. We discovered that $CD45^+$ cells in the tumor produced TNF-α in response to polyI:C (Fig. 3*A*). The major population of those $CD45^+$ cells was determined to be of $CD11b^+$ myeloid-lineage cells that coexpressed $F4/80^+$, $Gr1^+$, or $CD11c^+$. A small population of $NK1.1^+$ cells was also detected. $CD4^+$ T cells, $CD8^+$ T cells, and B cells were rarely detected in these implant tumors (Fig. S5*A*). Moreover, F4/80$^+$/Gr-$1^-$ cells were found to be the principal contributors to polyI:C-mediated TNF-α production (Fig. 3 *B* and *C*). $F4/80^+$ cells in 3LL tumor highly expressed macrophage mannose receptor (MMR; CD206), a M2 macrophage marker, in contrast to splenic F4/80$^+$CD11b$^+$ cells. Both TNF-α–producing and –nonproducing $F4/80^+$ cell populations in 3LL tumor showed indistinguishable levels of CD206 (Fig. S6), and dissimilar to MDSCs or splenic Mfs, as determined by the surface marker profiles (Table S3). Thus, the source of the TNF-α–producing cells in tumor is likely $F4/80^+$ Mfs with a TAM-like feature.

We harvested $F4/80^+$ cells from tumor samples extracted from WT and TICAM-$1^{-/-}$ mice at 30 min after polyI:C injection. These cells were used in in vitro experiments to verify the TNF-α–producing abilities and 3LL cytotoxicity properties (Fig. 4 *A* and *B*). WT $F4/80^+$ Mfs exhibited normal TNF-α–producing function and were able to kill 3LL cells upon exposure. This tumoricidal activity was ~50% neutralized by the addition of anti–TNF-α Ab (Fig. 4*C*), although incomplete inhibition by this mAb may reflect participation of other factors in TNF-α cytotoxicity. Furthermore, when active TNF-α protein (rTNF-α) was added exogenously to 3LL cell culture, the cytotoxic effects were still present and occurred in a dose-dependent manner (Fig. 4*D*). TNF-α–producing ability was also observed in $F4/80^+$ cells from implant tumor of MC38, B16D8, or EL4, and only the MC38 tumor was remediable by TICAM-1–derived TNF-α (Fig. S2 *B* and *C*). The MC38 tumor contained the F4/80$^+$/CD11b$^+$/Gr-$1^-$ cells, as in the 3LL tumor (Fig. S5*B*).

IFN-β did not enhance rTNF-α–mediated 3LL killing efficacy (Fig. S7*A*), a finding that was consistent with previously published data (29). No effect of IRF3/7 on polyI:C-induced 3LL tumor regression in vivo was confirmed using IRF3/7 double-knockout mice. However, polyI:C-dependent tumor regression was abrogated in 3LL-bearing IFN-α/β receptor (IFNAR)$^{-/-}$ mice (Fig. S7*B*). Quantitative PCR analysis of cells from WT vs. IFNAR$^{-/-}$ tumor-bearing mice revealed that the TLR3 level was basally low and not up-regulated in response to polyI:C in tumor-infiltrating $F4/80^+$ Mfs of IFNAR$^{-/-}$ mice (Fig. S7*C*). Accordingly, the TNF-α level was not up-regulated in tumor and serum in polyI:C-stimulated IFNAR$^{-/-}$ mice (Fig. S7*D*). Thus, basal induction of type I IFN serves as a critical factor for TLR3 function in tumor $F4/80^+$ Mfs to produce TNF-α in vivo. These results suggest that the direct effector for 3LL cytolysis by polyI:C involves TNF-α, which is derived from TICAM-1 downstream independent of the IRF3/7 axis. Our results indicate that cytotoxic TNF-α is produced via a distinct route from initial type I IFN and downstream of TICAM-1 in $F4/80^+$ TAM-like Mfs. Type I IFN do not synergistically act with TNF-α on 3LL killing, but is required to complete the TLR3/TICAM-1 pathway.

These results were confirmed by in vitro assay, wherein the $F4/80^+$ Mfs harvested from 3LL tumors in WT, TICAM-$1^{-/-}$, IPS-$1^{-/-}$, and TLR3$^{-/-}$ mice were stimulated with polyI:C (Fig. S8*A*). Both TNF-α release and 3LL cytotoxic abilities of polyI:C-stimulated $F4/80^+$ Mfs were specifically abrogated by the absence of TICAM-1 and TLR3 (Fig. S8 *A* and *B*). IPS-1 or

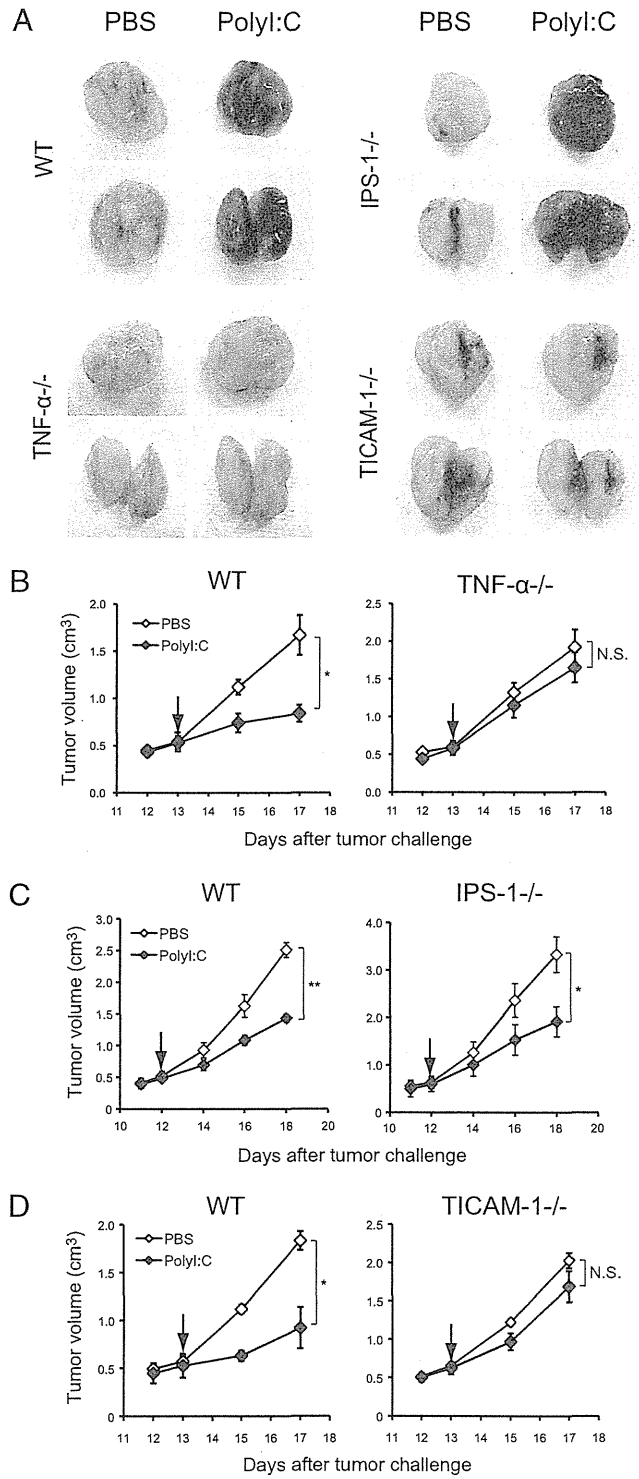


**Fig. 1.** Antitumor activity of polyI:C against 3LL tumor cells is mediated by the TICAM-1 pathway in vivo. (*A*) Representative photographs of 3LL tumors excised from WT, TNF-$\alpha^{-/-}$, TICAM-$1^{-/-}$, and IPS-$1^{-/-}$ mice. Whole tumor (*Upper*) and bisected tumor (*Lower*) are shown. (*B–D*) On day 0, 3LL tumor cells ($3 \times 10^6$) were s.c. implanted into B6 WT (*B–D*), TNF-$\alpha^{-/-}$ (*B*), TICAM-$1^{-/-}$ (*C*), and IPS-$1^{-/-}$ (*D*) mice. PolyI:C i.p. injection was started on the day indicated by arrow, then repeated every 4 d. Data are shown as tumor average size ± SE; $n = 3$–4 mice per group. $^*P < 0.05$; $^{**}P < 0.001$. N.S., not significant. A representative experiment of two with similar outcomes is shown.

MyD88 in F4/80$^+$ Mfs had no or minimal effect on the TNF-α tumoricidal effect against 3LL tumors. PolyI:C did not directly exert a cytotoxic effect on 3LL tumor cells (Fig. S8*C*).

**Role of the IPS-1 Pathway in F4/80$^+$ Cells.** Both TICAM-1 and IPS-1 are known to converge their signals on transcription factors NF-κB and IRF-3, which drive expression of TNF-α and IFN-β, respectively. PolyI:C-induced TNF-α production was reduced in F4/80$^+$ cells extracted from tumors of TICAM-$1^{-/-}$ mice, but not in samples of IPS-$1^{-/-}$ mice. We examined the expression of IFN-β in these cells after polyI:C stimulation. Compared with F4/80$^+$ cells from WT mice, IFN-β expression and production was barely decreased in IPS-$1^{-/-}$ F4/80$^+$ cells, but largely impaired in TICAM-$1^{-/-}$ F4/80$^+$ cells (Fig. S9*A*) as other cytokines tested. M1 Mf-associated cytokines/chemokines were generally reduced in TICAM-$1^{-/-}$ F4/80$^+$ cells compared with WT and IPS-$1^{-/-}$ cells >4 h after polyI:C stimulation (Fig. S9*A*), whereas M2 Mf-associated genes were barely affected by TICAM-1 disruption or polyI:C stimulation (Fig. S9*B*).

Most types of Mfs are known to express TLR3 in mice (30). Messages and proteins for type I IFN induction were conserved in the F4/80$^+$ tumor-infiltrating Mfs (Fig. S10 *A–C*). However, the TLR3 mRNA level was low in macrophage colony-stimulating factor (M-CSF)–derived Mfs compared with TAMs (Fig. S10*D*). We further examined whether IFN-β production might also have relied on the TICAM-1 pathway in other types of Mfs upon stimulation with polyI:C. In contrast to the F4/80$^+$ cells isolated from tumor (Fig. S11 *A* and *B*), the IPS-1 pathway was indispensable for polyI:C-mediated IFN-β production in mouse peritoneal Mfs and M-CSF–induced bone marrow-derived Mfs (Fig. S11 *C* and *E*). However, IPS-1 only slightly participated in polyI:C-mediated TNF-α production in these Mf subsets (Fig. S11 *D* and *F*). It appears then that the IPS-1 pathway is able to signal the presence of polyI:C and subsequently induce type I IFN. TICAM-1 is the protein that induces effective TNF-α in all subsets of Mfs.

**PolyI:C Influences Polarization of TAMs.** Plasticity is a characteristic feature of Mfs (25). Various factors and signals can influence polarization of Mf cells to induce the M1/M2 transition, which is accompanied by a substantial change in the Mf cell's expression profile of cytokines and chemokines. Previous studies have demonstrated that Mfs that have infiltrated into tumor are of the M2-polarized phenotype, which is known to contribute to tumor progression. To test the effects of polyI:C on the polarization of tumor-infiltrated Mf cells, we analyzed the gene expression profiles of these cells following in vitro polyI:C stimulation, and representative profiles were confirmed by quantitative PCR (Fig. 5 *A* and *B*). The mRNA expressions were increased for M1 Mf markers IL-12p40, IL-6, CXCL11, and IL-1β at 4 h after in vitro polyI:C treatment, as were mRNA levels of IFN-β and TNF-α and ex vivo results. The M2 Mf markers arginase-1 (*Arg1*), chitinase 3-like 3 (*Chi3l3*), and MMR (*Mrc1*) were unchanged, compared with unstimulated levels; however, the M2 Mf marker IL-10, a regulatory cytokine, was induced. In addition, there was no difference observed in the mRNA expression levels of MMP9 (*Mmp9*) and VEGFA (*Vegfa*), both of which are involved in tissue remodeling and angiogenesis events of tumor progression (Fig. 5*C*). The polyI:C-induced M1 markers and IL-10 expression that were upregulated in WT and IPS-$1^{-/-}$ F4/80$^+$ cells were found to be abrogated in TICAM-$1^{-/-}$ F4/80$^+$ cells (Fig. 5 *A* and *B*), reinforcing the results obtained with F4/80$^+$ Mfs isolated from 3LL tumors in mice injected with polyI:C (Fig. S9 *A* and *B*). It appears that TICAM-1 is responsible for the M1 polarization of F4/80$^+$ Mf cells in tumors, but has no effect on M2 markers. We further examined the expression of IRF-5 and IRF-4, which are considered the master regulators for M1 and M2 polarization, respectively (31, 32). As expected, polyI:C induced IRF-5 mRNA expression, but had no effect on IRF-4 mRNA expression in vitro (Fig. 5 *A* and *B*). Jmjd3, a histone H3K27 demethylase involved in IRF-4 expression, is reportedly induced by TLR stimulation (33). In our study, polyI:C stimulation increased Jmjd3 mRNA in F4/80$^+$ cells

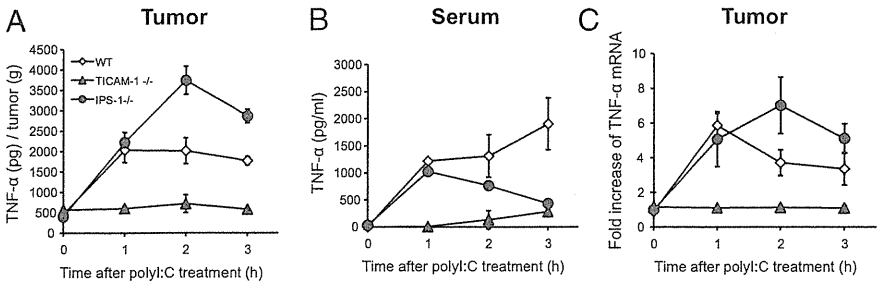


**Fig. 2.** TNF-α production in tumor and serum of polyI:C-injected 3LL tumor-bearing mice. Mice bearing 3LL tumor were i.p. injected with 200 μg polyI:C. Tumor (*A*) and serum (*B*) were collected at 0, 1, 2, and 3 h after polyI:C injection, and TNF-α concentration was determined by ELISA. TNF-α level in tumor is presented as [TNF-α protein (pg)/tumor weight (g)]. (*C*) Tumors were isolated from polyI:C-injected tumor-bearing WT, TICAM-1$^{-/-}$, and IPS-1$^{-/-}$ mice, and TNF-α mRNA was measured by quantitative PCR; $n$ = 3. Data are shown as average ± SD. A representative experiment of two with similar outcomes is shown.

(Fig. 5*B*). The polyI:C-triggered M1 gene expression continued long in tumor-infiltrated Mfs, a finding that may further explain the tumor-suppressing feature of these Mfs, in addition to the concern of early inducing TNF-α.

## Discussion

In this study we demonstrated that the tumor-supporting properties of tumor-infiltrating F4/80$^+$ Mfs characterized by M2 markers are dynamic and able to shift to an M1-dominant state upon the particular signal provided by PRRs. In 3LL tumors that express minimal amounts of MHC class I/II and recruit a large amount of myeloid cells, F4/80$^+$ Mfs function to sustain the tumor in the surrounding microenvironment. This tumor-supporting environment can be disrupted by stimulation with an RNA duplex through a TICAM-1 signal and subsequent induction of mediators such as TNF-α. Thus, the TICAM-1 signal in tumor-infiltrating Mfs plays a key role in TNF-α and M1 shift-mediated tumor regression. These results were confirmed using another cell line, MC38 colon adenocarcinoma (34), although MC38 cells express MHC class I. B16D8 melanoma (12) and EL4 lymphoma (35) were resistant to TNF-α, but their F4/80$^+$ Mfs still possessed TNF-α–inducing potential by stimulation with polyI:C; their susceptibilities to polyI:C reportedly depend on other effectors (12, 35). These results may partly explain the reported findings that tumors regressed in patients with simultaneous virus infection (36, 37), and that tumor growth was inhibited by polyI:C injection in tumor-bearing mice (6, 7).

In contrast, polyI:C-stimulated PEC or bone marrow-derived Mfs induce type I IFN via the IPS-1 pathway unlike the case of tumor-infiltrating F4/80$^+$ Mfs. Nevertheless, all of these Mf subsets produce proinflammatory cytokines, including TNF-α, in a TICAM-1–dependent manner. Thus, the key question that arose was why predominant TICAM-1 dependence for polyI:C-mediated production of TNF-α occurred in F4/80$^+$ tumor-infiltrating Mfs leading to tumor regression. A marked finding is that the TLR3 protein level is high in tumor-infiltrating Mfs compared with other sources of Mfs (Fig. S10). In addition, the IPS-1 pathway is unresponsive to polyI:C if the polyI:C is exogenously added to the tumor-infiltrating Mfs without transfection reagents. The cytoplasmic dsRNA sensors normally work for IFN induction in tumor F4/80$^+$ Mfs if the polyI:C is transfected into the cells. TICAM-1–dependent TNF-α production by F4/80$^+$ Mfs (Fig. S11 *D* and *F*) occurs partly because F4/80$^+$ Mfs express a high basal level of TLR3 and fail to take up extrinsic polyI:C into the cytoplasm. Of many subsets of Mfs, these properties (38) are unique to the F4/80$^+$ Mfs.

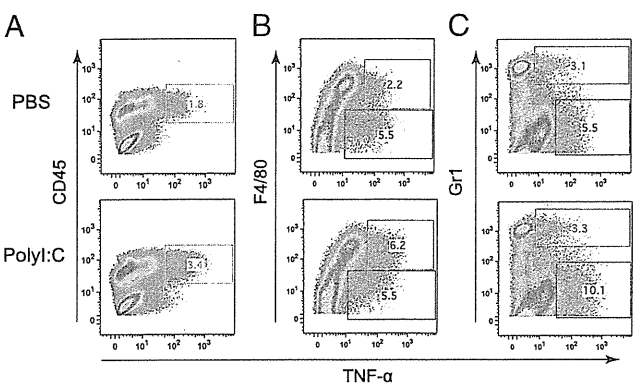


**Fig. 3.** F4/80$^+$ cells are responsible for the polyI:C-induced elevation of TNF-α production in tumor. Mice bearing 3LL tumors were i.p. injected with 200 μg polyI:C. TNF-α–producing cells in tumors of polyI:C- or PBS-injected mice were examined by immunohistochemical staining and flow cytometry to determine intracellular cytokine expression profiles of CD45$^+$ cells (*A*), F4/80$^+$ cells (*B*), and Gr1$^+$ cells (*C*). CD45$^+$ cells in tumor were gated and are shown in *B* and *C*. A representative experiment of two with similar outcomes is shown. TNF-α$^+$ gating squares are shown in red (positive) and green (negative).

Hemorrhagic necrosis and tumor size reduction are closely correlated with constitutive production of TNF-α (39, 40). The association of PRR-derived TNF-α and hemorrhagic necrosis of tumor has been described earlier. Carswell et al. (41) showed that TNF-α is robustly expressed in mouse serum following treatment with bacillus Calmette–Guérin and endotoxin. Bioassay of TNF-α as reflected by the degree of hemorrhagic necrosis of transplanted Meth A sarcoma in BALB/c mice led the authors to speculate that Mfs are responsible for TNF-α induction. Many years later, Dougherty et al. (42) identified the mechanism responsible for the TNF-α production associated with antitumor activity; macrophages isolated from tumors in mice with inactivating mutation in the TLR4 gene [Lps(d) in C3H/HeJ] expressed 5- to 10-fold less TNF-α than tumors in WT mice. This finding represents a unique recognition of a PRR contributing to the cancer phenotype. Subsequent studies determined that MyD88 is involved in the induction of TNF-α via TLR4 binding to its cognate ligand, lipid A endotoxin (15, 43). Because the TLR3 signal is independent of MyD88, this MyD88 concept is not applicable to the present study on polyI:C-dependent tumor regression.

Alternatively, endotoxin/lipid A may have activated TICAM-1 in previous reports on TLR4-derived TNF-α because TLR4 can recruit TICAM-1 in addition to MyD88 (15). The lipid A derivative monophospholipid A preferentially activates the TICAM-1 pathway of TLR4 (43). It is likely that TICAM-1 participates in TLR4-mediated tumor regression in addition to MyD88, although MyD88 is not involved in the polyI:C signaling. This point was further proven using TNF-α$^{-/-}$ mice: TICAM-1–derived TNF-α in F4/80$^+$ Mf cells has a critical role in the induction of tumor necrosis and regression by polyI:C. The results are consistent with the finding that both TICAM-1 and IPS-1 pathways are able to induce NF-κB activation secondary to polyI:C stimulation, and indeed their signals converge at the IκB kinase complex (18).

TICAM-1 is able to induce many of the IFN-inducible genes that MyD88 cannot in mDCs (44). In both cases of TICAM-1 and MyD88 stimulation, tumor-infiltrating Mfs facilitate the expression of many genes in addition to TNF-α. The M2 phenotype of F4/80$^+$ Mfs or tumor-associated Mfs is modified dependent on these additional factors. IFNAR facilitates polyI:C-mediated tumor regression in tumor-bearing mice, lack of which results in no induction of TLR3 (Fig. S7). Thus, preceding the polyI:C

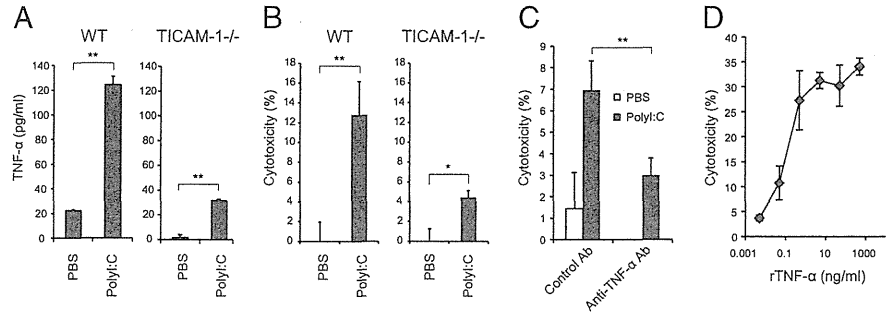


**Fig. 4.** Poly I:C enhances TNF-α production and cytotoxicity of F4/80$^+$ cells in tumor. Poly I:C (200 μg) or PBS was i.p. injected into 3LL tumor-bearing WT mice. After 30 min, F4/80$^+$ cells isolated from tumor were cultured for 24 h and TNF-α concentration in the conditioned medium was determined by ELISA (*A*). In parallel, the cytotoxicity of tumor-infiltrating F4/80$^+$ cells against 3LL tumor cells was measured by $^{51}$Cr-release assay (*B*). Anti–TNF-α neutralization antibody or control antibody was added (10 μg/mL) to mixed culture of isolated tumor-infiltrating F4/80$^+$ cells and 3LL tumor cells (*C*). (*D*) Cytotoxic activity of TNF-α against 3LL tumor cells. Recombinant TNF-α was added to $^{51}$Cr-labeled 3LL tumor cell culture at various concentrations. After 20 h, cytotoxicity was measured; $n = 3$. Data are shown as average ± SD. $*P < 0.05$, $**P < 0.001$. A representative experiment of three with similar outcomes is shown.

response, minute type I IFN of undefined source has to be provided to set the TLR3/TICAM-1 pathway, which may primarily fail in IFNAR$^{-/-}$ mice. Cellular effectors, cytotoxic T lymphocyte (CTL) and NK cells, are induced secondary to activation of IFN-inducible genes in a late phase of polyI:C-stimulated myeloid cells (45–47). The relationship among the TICAM-1–mediated type I IFN liberation, these late-phase effectors, and tumor regression remains an open question in this setting.

M1 Mf cells function to protect the host against tumors by producing large amounts of inflammatory cytokines and activating the immune response (48, 49). However, distinct types of M2 cells differentiate when monocytes are stimulated with IL-4 and IL-13 (M2a), immune complexes/TLR ligands (M2b), or IL-10 and glucocorticoids (M2c) (50). In our study, polyI:C stimulation led to incremental expression of the M1 Mf-related genes. In contrast, polyI:C stimulation was not associated with M2 polarization, except for IL-10. Other genes related to angiogenesis and extravasation were not affected by polyI:C treatment. Thus, polyI:C was able to induce the characteristic M1 conversion and, in turn, contribute to tumor regression. It is notable that TAM cells usually have defective and delayed NF-κB activation in response to different proinflammatory signals, such as expression of cytotoxic mediators NO, cytokines, TNF-α, and IL-12 (51–53). These observations are in apparent contrast with the function of other resident Mf species. This discrepancy may again reflect a dynamic change in the tumor microenvironment during tumor progression.

In line with our findings, virus infection has been observed to instigate tumor regression in patients with cancer (36, 54). Gene therapy for cancer patients using virus-derived vectors has proved effective in reducing tumors in clinic (36, 37). Administration of dsRNA elicits IFN induction, NK cell activation, and CTL proliferation for antitumor effectors in vivo (19, 55). This is a unique finding that tumor-infiltrating Mfs are a target of dsRNA and converted from tumor supporters to tumoricidal effectors. Hence, the antitumor effect of dsRNA adjuvant is ultimately based on the liberation of type I IFN, functional maturation of mDCs, and modulation of tumor-infiltrating Mfs, where TICAM-1 is a crucial transducer in eliciting antitumor immunity.

## Methods

Inbred C57BL/6 WT mice were purchased from CLEA Japan, Inc. TICAM-1$^{-/-}$ and IPS-1$^{-/-}$ mice were generated in our laboratory and maintained as described previously. IRF-3/7 double-KO mice were a gift from T. Taniguchi

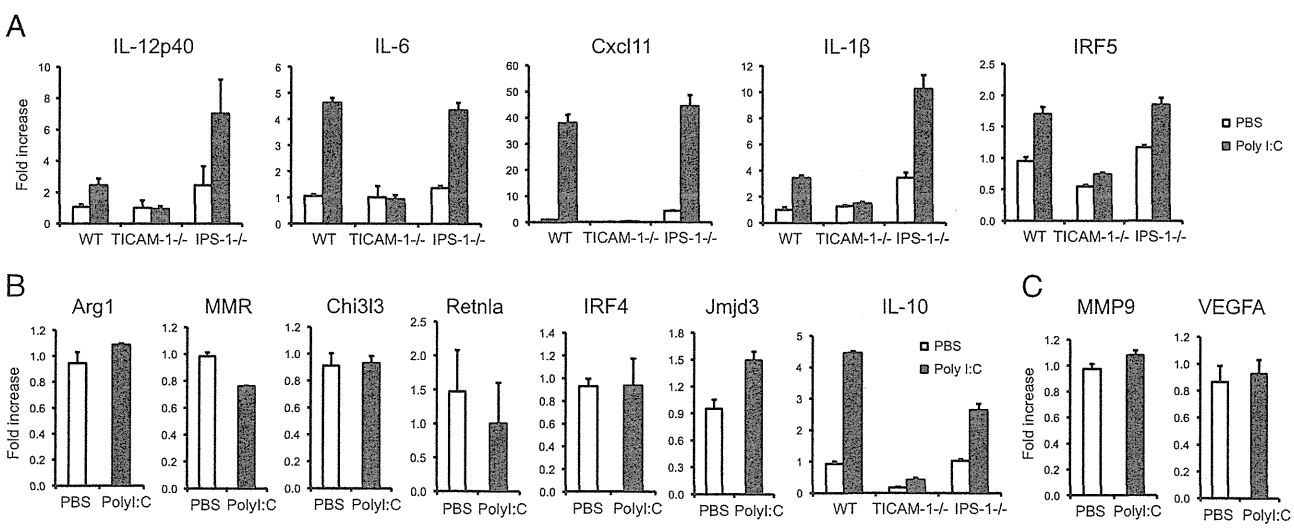


**Fig. 5.** Poly I:C induces M1 polarization of TAMs. F4/80$^+$ cells were isolated from 3LL tumor and stimulated with poly I:C (50 μg/mL) for 4 h. Total RNA was extracted and used to analyze the transcript expression levels of M1 (*A*) and M2 (*B* and *C*) markers; $n = 3$. Data are shown as average ± SD. A representative experiment of two with similar outcomes is shown.

(University of Tokyo, Tokyo, Japan). TNF-$\alpha^{-/-}$ mice were kindly provided by A. Nakane (Hirosaki University, Aomori, Japan) and Y. Iwakura (University of Tokyo). Mice 6–10 wk of age were used in all experiments. 3LL lung cancer cells were cultured at 37 °C under 5% $CO_2$ in RPMI containing 10% FCS, penicillin, and streptomycin. This study was carried out in strict accordance with the recommendations in the Guide for the Care and Use of Laboratory Animals of the National Institutes of Health. The protocol was approved by the Committee on the Ethics of Animal Experiments in the Animal Safety Center, Hokkaido University, Japan. All mice were used according to the guidelines of the Institutional Animal Care and Use Committee of Hokkaido University, who approved this study as no. 08-0290, "Analysis of Anti-Tumor Immune Response Induced by the Activation of Innate Immunity."

Other detailed methods are provided in *SI Methods*.

**ACKNOWLEDGMENTS.** We thank Dr. T. Taniguchi (University of Tokyo) and D. M. Segal (EIB/NCI, Bethesda, MD) for kindly providing us with IRF-3/7 double KO mice and mAb against mouse TLR3. This work was supported in part by Grants-in-Aid from the Ministry of Education, Science, and Culture (MEXT), "the Carcinogenic Spiral" a MEXT Grant-in-Project, and the Ministry of Health, Labor, and Welfare of Japan, the Takeda Foundation, the Akiyama Foundation, and the Waxman Foundation.

1. Grivennikov SI, Greten FR, Karin M (2010) Immunity, inflammation, and cancer. *Cell* 140:883–899.
2. de Visser KE, Eichten A, Coussens LM (2006) Paradoxical roles of the immune system during cancer development. *Nat Rev Cancer* 6:24–37.
3. Chan AT, Ogino S, Fuchs CS (2007) Aspirin and the risk of colorectal cancer in relation to the expression of COX-2. *N Engl J Med* 356:2131–2142.
4. Rakoff-Nahoum S, Medzhitov R (2007) Regulation of spontaneous intestinal tumorigenesis through the adaptor protein MyD88. *Science* 317:124–127.
5. Chen GY, Shaw MH, Redondo G, Núñez G (2008) The innate immune receptor Nod1 protects the intestine from inflammation-induced tumorigenesis. *Cancer Res* 68: 10060–10067.
6. Sarma PS, Shiu G, Neubauer RH, Baron S, Huebner RJ (1969) Virus-induced sarcoma of mice: Inhibition by a synthetic polyribonucleotide complex. *Proc Natl Acad Sci USA* 62: 1046–1051.
7. Levy HB, Law LW, Rabson AS (1969) Inhibition of tumor growth by polyinosinic-polycytidylic acid. *Proc Natl Acad Sci USA* 62:357–361.
8. Absher M, Stinebring WR (1969) Toxic properties of a synthetic double-stranded RNA. Endotoxin-like properties of poly I. poly C, an interferon stimulator. *Nature* 223: 715–717.
9. Talmadge JE, et al. (1985) Immunomodulatory effects in mice of polyinosinic-polycytidylic acid complexed with poly-L-lysine and carboxymethylcellulose. *Cancer Res* 45: 1058–1065.
10. Longhi MP, et al. (2009) Dendritic cells require a systemic type I interferon response to mature and induce $CD4^+$ Th1 immunity with poly IC as adjuvant. *J Exp Med* 206: 1589–1602.
11. Matsumoto M, Seya T (2008) TLR3: Interferon induction by double-stranded RNA including poly(I:C). *Adv Drug Deliv Rev* 60:805–812.
12. Akazawa T, et al. (2007) Antitumor NK activation induced by the Toll-like receptor 3-TICAM-1 (TRIF) pathway in myeloid dendritic cells. *Proc Natl Acad Sci USA* 104: 252–257.
13. Miyake T, et al. (2009) Poly I:C-induced activation of NK cells by CD8 $alpha^+$ dendritic cells via the IPS-1 and TRIF-dependent pathways. *J Immunol* 183:2522–2528.
14. McCartney S, et al. (2009) Distinct and complementary functions of MDA5 and TLR3 in poly(I:C)-mediated activation of mouse NK cells. *J Exp Med* 206:2967–2976.
15. Oshiumi H, Matsumoto M, Funami K, Akazawa T, Seya T (2003) TICAM-1, an adaptor molecule that participates in Toll-like receptor 3-mediated interferon-beta induction. *Nat Immunol* 4:161–167.
16. Yoneyama M, et al. (2005) Shared and unique functions of the DExD/H-box helicases RIG-I, MDA5, and LGP2 in antiviral innate immunity. *J Immunol* 175:2851–2858.
17. Takeuchi O, Akira S (2010) Pattern recognition receptors and inflammation. *Cell* 140: 805–820.
18. Sasai M, et al. (2006) NAK-associated protein 1 participates in both the TLR3 and the cytoplasmic pathways in type I IFN induction. *J Immunol* 177:8676–8683.
19. Seya T, Matsumoto M (2009) The extrinsic RNA-sensing pathway for adjuvant immunotherapy of cancer. *Cancer Immunol Immunother* 58:1175–1184.
20. Iwasaki A, Medzhitov R (2010) Regulation of adaptive immunity by the innate immune system. *Science* 327:291–295.
21. Condeelis J, Pollard JW (2006) Macrophages: Obligate partners for tumor cell migration, invasion, and metastasis. *Cell* 124:263–266.
22. Schuler G, Schuler-Thurner B, Steinman RM (2003) The use of dendritic cells in cancer immunotherapy. *Curr Opin Immunol* 15:138–147.
23. Murdoch C, Muthana M, Coffelt SB, Lewis CE (2008) The role of myeloid cells in the promotion of tumour angiogenesis. *Nat Rev Cancer* 8:618–631.
24. Borrello MG, Degl'Innocenti D, Pierotti MA (2008) Inflammation and cancer: The oncogene-driven connection. *Cancer Lett* 267:262–270.
25. Biswas SK, Mantovani A (2010) Macrophage plasticity and interaction with lymphocyte subsets: Cancer as a paradigm. *Nat Immunol* 11:889–896.
26. Farma JM, et al. (2007) Direct evidence for rapid and selective induction of tumor neovascular permeability by tumor necrosis factor and a novel derivative, colloidal gold bound tumor necrosis factor. *Int J Cancer* 120:2474–2480.
27. Masuda H, et al. (2002) High levels of RAE-1 isoforms on mouse tumor cell lines assessed by the anti-pan-Rae-1 polyclonal antibody confers tumor cell cytotoxicity on mouse NK cells. *Biochem Biophys Res Commun* 290:140–145.
28. Smyth MJ, et al. (2004) NKG2D recognition and perforin effector function mediate effective cytokine immunotherapy of cancer. *J Exp Med* 200:1325–1335.
29. Remels L, Fransen L, Huygen K, De Baetselier P (1990) Poly I:C activated macrophages are tumoricidal for TNF-α-resistant 3LL tumor cells. *J Immunol* 144:4477–4486.
30. Jelinek I, et al. (2011) TLR3-specific double-stranded RNA oligonucleotide adjuvants induce dendritic cell cross-presentation, CTL responses, and antiviral protection. *J Immunol* 186:2422–2429.
31. Krausgruber T, et al. (2011) IRF5 promotes inflammatory macrophage polarization and TH1-TH17 responses. *Nat Immunol* 12:231–238.
32. Satoh T, et al. (2010) The Jmjd3-*Irf4* axis regulates M2 macrophage polarization and host responses against helminth infection. *Nat Immunol* 11:936–944.
33. De Santa F, et al. (2007) The histone H3 lysine-27 demethylase Jmjd3 links inflammation to inhibition of polycomb-mediated gene silencing. *Cell* 130:1083–1094.
34. Zitvogel L, et al. (1995) Cancer immunotherapy of established tumors with IL-12. Effective delivery by genetically engineered fibroblasts. *J Immunol* 155:1393–1403.
35. Abe R, Peng T, Sailors J, Bucala R, Metz CN (2001) Regulation of the CTL response by macrophage migration inhibitory factor. *J Immunol* 166:747–753.
36. Russell SJ (2002) RNA viruses as virotherapy agents. *Cancer Gene Ther* 9:961–966.
37. Aghi M, Martuza RL (2005) Oncolytic viral therapies—the clinical experience. *Oncogene* 24:7802–7816.
38. Watanabe A, et al. (2011) Raftlin is involved in the nucleocapture complex to induce poly(I:C)-mediated TLR3 activation. *J Biol Chem* 286:10702–10711.
39. Mocellin S, Rossi CR, Pilati P, Nitti D (2005) Tumor necrosis factor, cancer and anticancer therapy. *Cytokine Growth Factor Rev* 16:35–53.
40. Balkwill F (2009) Tumour necrosis factor and cancer. *Nat Rev Cancer* 9:361–371.
41. Carswell EA, et al. (1975) An endotoxin-induced serum factor that causes necrosis of tumors. *Proc Natl Acad Sci USA* 72:3666–3670.
42. Dougherty ST, Eaves CJ, McBride WH, Dougherty GJ (1997) Molecular mechanisms regulating TNF-alpha production by tumor-associated macrophages. *Cancer Lett* 111: 27–37.
43. Mata-Haro V, et al. (2007) The vaccine adjuvant monophosphoryl lipid A as a TRIF-biased agonist of TLR4. *Science* 316:1628–1632.
44. Ebihara T, et al. (2010) Identification of a polyI:C-inducible membrane protein that participates in dendritic cell-mediated natural killer cell activation. *J Exp Med* 207: 2675–2687.
45. Akazawa T, et al. (2004) Adjuvant-mediated tumor regression and tumor-specific cytotoxic response are impaired in MyD88-deficient mice. *Cancer Res* 64:757–764.
46. Akazawa T, et al. (2007) Tumor immunotherapy using bone marrow-derived dendritic cells overexpressing Toll-like receptor adaptors. *FEBS Lett* 581:3334–3340.
47. Schulz O, et al. (2005) Toll-like receptor 3 promotes cross-priming to virus-infected cells. *Nature* 433:887–892.
48. Mantovani A, Sica A, Locati M (2007) New vistas on macrophage differentiation and activation. *Eur J Immunol* 37:14–16.
49. Martinez FO, Helming L, Gordon S (2009) Alternative activation of macrophages: An immunologic functional perspective. *Annu Rev Immunol* 27:451–483.
50. Mantovani A, et al. (2004) The chemokine system in diverse forms of macrophage activation and polarization. *Trends Immunol* 25:677–686.
51. Sica A, et al. (2000) Autocrine production of IL-10 mediates defective IL-12 production and NF-kappa B activation in tumor-associated macrophages. *J Immunol* 164:762–767.
52. Torroella-Kouri M, et al. (2005) Diminished expression of transcription factors nuclear factor kappaB and CCAAT/enhancer binding protein underlies a novel tumor evasion mechanism affecting macrophages of mammary tumor-bearing mice. *Cancer Res* 65: 10578–10584.
53. Biswas SK, et al. (2006) A distinct and unique transcriptional program expressed by tumor-associated macrophages (defective NF-kappaB and enhanced IRF-3/STAT1 activation). *Blood* 107:2112–2122.
54. Bluming AZ, Ziegler JL (1971) Regression of Burkitt's lymphoma in association with measles infection. *Lancet* 2:105–106.
55. Matsumoto M, Oshiumi H, Seya T (2011) Antiviral responses induced by the TLR3 pathway. *Rev Med Virol* 21:67–77.

# Supporting Information

Shime et al. 10.1073/pnas.1113099109

## SI Methods

**Reagents.** PolyI:C was purchased from GE Healthcare, which was free from LPS contamination. TNF-α and IFN-β ELISA kit was purchased from eBioscience and PBL InterferonSource, respectively. Recombinant TNF-α was purchased from R&D Systems.

**Tumor Cells and Tumor-Infiltrated Immune Cells.** We first tested the amounts of macrophages (Mfs) in implant tumors formed in B6 mice. Mouse lymphoma (EL4), Lewis lung carcinoma (3LL), adenocarcinoma MC38, and melanoma (B16D8) lines grew well in the back of mice, and the Mf content was maximal in the 3LL tumor. MC38, a murine colon adenocarcinoma cell line, was a gift from S. A. Rosenberg (National Cancer Institute, Bethesda) (1). Hemorrhagic necrosis shown in Fig. 1*A* was typically induced in response to polyI:C in 3LL tumor. We then used the 3LL line for this study.

3LL cells were found to express very low amounts of detectable MHC class I or class II (Table S1), suggesting this cell type as a possible target for natural killer (NK) cells but not cytotoxic T lymphocytes (CTLs). 3LL cells were found to express appreciable amounts of the NKG2D ligand, retinoic acid-inducible gene 1, consistent with previous reports (Table S1) (2, 3). 3LL cells also expressed mRNA transcripts for Toll-like receptor 3 (TLR3), Toll–IL-1 receptor domain-containing adaptor molecule 1 (TICAM-1), IFN-β promoter stimulator 1 (IPS-1), and melanoma differentiation-associated protein 5 (MDA5). Exposure to polyI:C-stimulated peritoneal Mfs caused significant death of 3LL cells, which was likely an effect of liberated inflammatory cytokines such as TNF-α (4). Consistent with previously reported data about 3LL properties in vitro, the 3LL cells we used were not damaged by direct polyI:C treatment or exposure to 3LL-derived cytokines (Fig. S8*C*). When 3LL cells were implanted s.c. in mice, the resulting tumors were found to contain a high amount (>30%) of $CD45.2^+$ cells (Fig. S5*A*). The major population of those $CD45.2^+$ cells was determined to be of $CD11b^+$ myeloid lineage cells that coexpressed $F4/80^+$, $Gr1^+$, or $CD11c^+$. A small population of $NK1.1^+$ cells was also detected. $CD4^+$ T cells, $CD8^+$ T cells, and B cells were rarely detected in these implant tumors (Fig. S5*A*).

**Cytotoxic Activity Assay.** Mice bearing 3LL tumor were injected i.p. with polyI:C. Mice were killed and $F4/80^+$ cells were isolated from tumor by using MACS-positive selection beads (Miltenyi) as described previously. 3LL cells were labeled with $^{51}Cr$ for 3–5 h and then washed three times with the medium. $F4/80^+$ cells, and 3LL cells were cocultured at the indicated ratio. After 20 h, supernatants were harvested and $^{51}Cr$ release was measured in each sample. Specific lysis was calculated by the following formula: cytotoxicity (%) = [(experimental release − spontaneous release)/(max release − spontaneous release)] × 100.

**Flow Cytometric Analysis.** Mononuclear cells prepared from spleen and tumor were treated with anti-CD16/32 (no. 93) and stained with APC–anti-CD45.2 (no. 104), FITC–anti-CD11b (M1/70), PE–anti-GR1 (RB6-8C5), FITC–anti-CD11c (N418), PE– or APC–anti-F4/80 (BM8), PE–anti-NK1.1 (PK136), PE–anti-CD49b (DX5), PE–anti-CD3e (145-2C11), FITC–anti-CD4 (GK1.5), FITC–anti-CD8a (53-6.7), and PE- and anti-CD19 (MB19-1; eBioscience and Biolegend; Table S2). Samples were analyzed with FACSCalibur (BD Biosciences), and data analysis was performed using FlowJo software (Tree Star). For intracellular cytokine staining, we freshly isolated tumors from polyI:C or PBS-injected mice at 1 h and incubated the cells in the presence of 10 μg/mL Brefeldin A for 3 h. Cells were fixed and stained with the combination of anti-CD45.2 Ab and anti-F4/80 Ab or anti-Gr1 Ab, followed by permeabilizing and staining with anti-TNF Ab using BD Cytofix/Cytoperm Kit (BD Biosciences).

**Quantitative PCR Analysis.** Tumor samples were cut into small pieces and homogenized with TRIzol Reagent (Invitrogen). Total RNA was isolated according to the manufacturer's instruction. Reverse transcription was performed using High-Capacity cDNA Reverse Transcription Kit (Applied Biosystems). Real-time PCR was performed with Power SYBR Green PCR Master Mix (Applied Biosystems) with a StepOne Real-Time PCR System (Applied Biosystems). Expression of the cytokine gene was normalized to the expression of *GAPDH*. We used primer pairs listed in Table S3. Data were analyzed by the ΔΔCt method.

**ELISA and Cytokine Beads Assay.** Tumor samples were cut into small pieces and homogenized with CelLytic MT Mammalian Tissue Lysis/Extraction Reagent (Sigma) supplemented with Complete Protease Inhibitor Mixture (Roche) on ice. Lysate was centrifuged to remove insoluble materials, and the supernatant was used for ELISA. Serum cytokine concentration was determined by ELISA or cytokine bead assays. Data were shown as TNF-α (pg) per weight of tumor (g).

**Histochemistry and Immunohistochemistry.** 3LL tumor was fixed with buffered 10% formalin overnight and embedded in paraffin wax, and sections 4 μm in thickness were stained with H&E. For immunohistochemistry, tumor was embedded in optimal cutting-temperature compound, and snap-frozen in liquid nitrogen. Cryosections 6 μm in thickness were air-dried for 60 min and fixed for 15 min with prechilled acetone and then incubated with FITC–anti-CD31 antibody (390; BioLegend). The sections were mounted in Prolong Gold Antifade Reagent with DAPI (Invitrogen). Images were obtained with a Leica LSM510 confocal laser-scanning microscope.

**Tumor Challenge and PolyI:C Treatment.** Mice were shaved at the back and injected s.c with 200 μL of $3 \times 10^6$ 3LL cells in PBS(−). Tumor size was measured using a caliper. Tumor volume was calculated using the following formula: tumor volume ($cm^3$) = (long diameter) × (short diameter)$^2$ × 0.4. PolyI:C (250 μg/head) with no detectable LPS was injected i.p. as indicated. In some cases, polymixin B-treated polyI:C was used. When an average tumor volume of 0.5–0.8 $cm^3$ was reached, the treatment was started and repeated every 4 d.

**Isolation of $F4/80^+$ Cells from Tumor.** Tumors formed by 3LL cells were excised at 2 wk after transplantation and treated with 0.05 mg/mL Collagenase I (Sigma), 0.05 mg/mL Collagenase IV (Sigma), 0.025 mg/mL hyaluronidase (Sigma), and 0.01 mg/mL DNase I (Roche) in HBSS at 37 °C for 10 min. $F4/80^+$ cells were isolated by using biotinylated anti-F4/80 antibody (BM8) and Streptavidin MicroBeads (Miltenyi). We routinely prepared $F4/80^+$ cells at >90% purity from tumor.

1. Zitvogel L, et al. (1995) Cancer immunotherapy of established tumors with IL-12. Effective delivery by genetically engineered fibroblasts. *J Immunol* 155:1393–1403.
2. Masuda H, et al. (2002) High levels of RAE-1 isoforms on mouse tumor cell lines assessed by the anti-pan-Rae-1 polyclonal antibody confers tumor cell cytotoxicity on mouse NK cells. *Biochem Biophys Res Commun* 290:140–145.
3. Smyth MJ, et al. (2004) NKG2D recognition and perforin effector function mediate effective cytokine immunotherapy of cancer. *J Exp Med* 200:1325–1335.
4. Remels L, Fransen L, Huygen K, De Baetselier P (1990) Poly I:C activated macrophages are tumoricidal for TNF-α-resistant 3LL tumor cells. *J Immunol* 144:4477–4486.

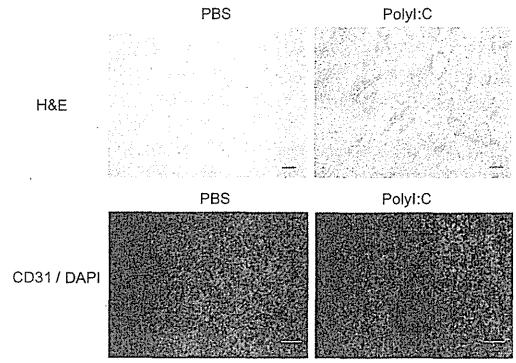


**Fig. S1.** Poly I:C induces hemorrhagic necrosis of tumor. 3LL tumor-bearing mice were i.p. injected with 200 μg poly I:C and tumors were isolated 12 h later. Formalin-fixed tumors stained with H&E (*Upper*) and frozen sections stained with anti-CD31 antibody and DAPI nuclear stain (*Lower*). Original magnification 10× for all panels. (Scale bars, 100 μm.) A representative experiment of three with similar outcomes is shown.

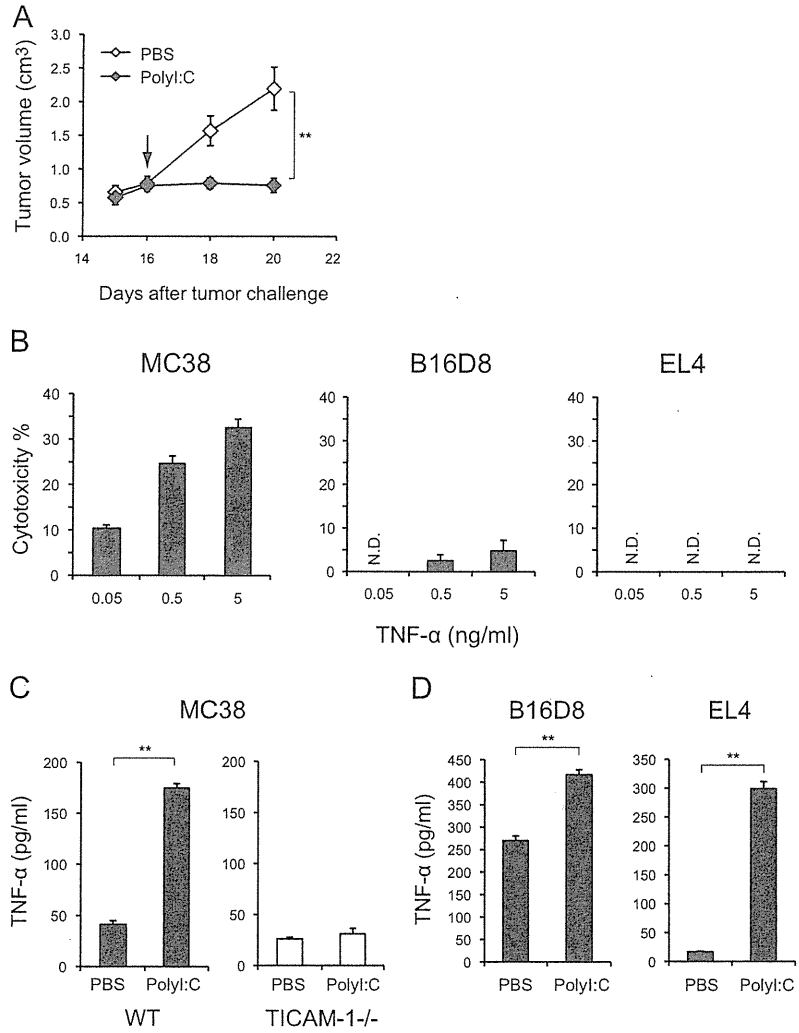


**Fig. S2.** Poly:C induces TNF-α production by tumor-associated F4/80$^+$ Mfs in various types of tumor. (*A*) MC38 cells ($1 \times 10^5$) were s.c implanted into C57BL/6 mice (day 0). Poly:C (200 μg) was i.p. injected on day 16. Data are shown as tumor average size ± SE; $n = 3$–4 mice per group. (*B*) Sensitivity of MC38, B16D8, and EL4 cells to recombinant TNF-α. (*C* and *D*) MC38, B16D8, and EL4 tumor-bearing mice were i.p injected with 200 μg poly:C. After 1 h, F4/80$^+$ cells were isolated from tumors and incubated for 24 h. TNF-α concentration in the conditioned medium was determined by ELISA; $n = 3$. Data are shown as average ± SD. N.D., not detected. A representative experiment of two with similar outcomes is shown.

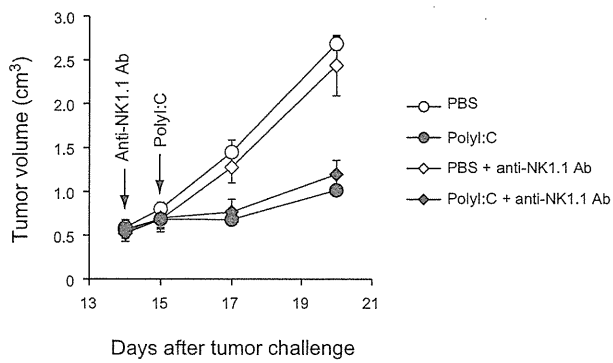


**Fig. S3.** NK cells are not essential for poly:C-induced antitumor activity in vivo. 3LL tumor cells ($3 \times 10^6$) were s.c transplanted into C57BL/6 mice (day 0). NK cells were depleted by injection of anti-NK1.1 antibody (PK136) into 3LL tumor-bearing mice on day 14. All doses of antibody and treatment regimens were determined in preliminary studies using the same lot of antibodies used for the experiments. Treatment was confirmed to deplete completely the desired cell populations for the entire duration of the study. Poly:C (250 μg) was i.p injected on day 15 and the tumor volume was measured. Data shown are means ± SE, $n = 3$. A representative experiment of two with similar outcomes is shown.

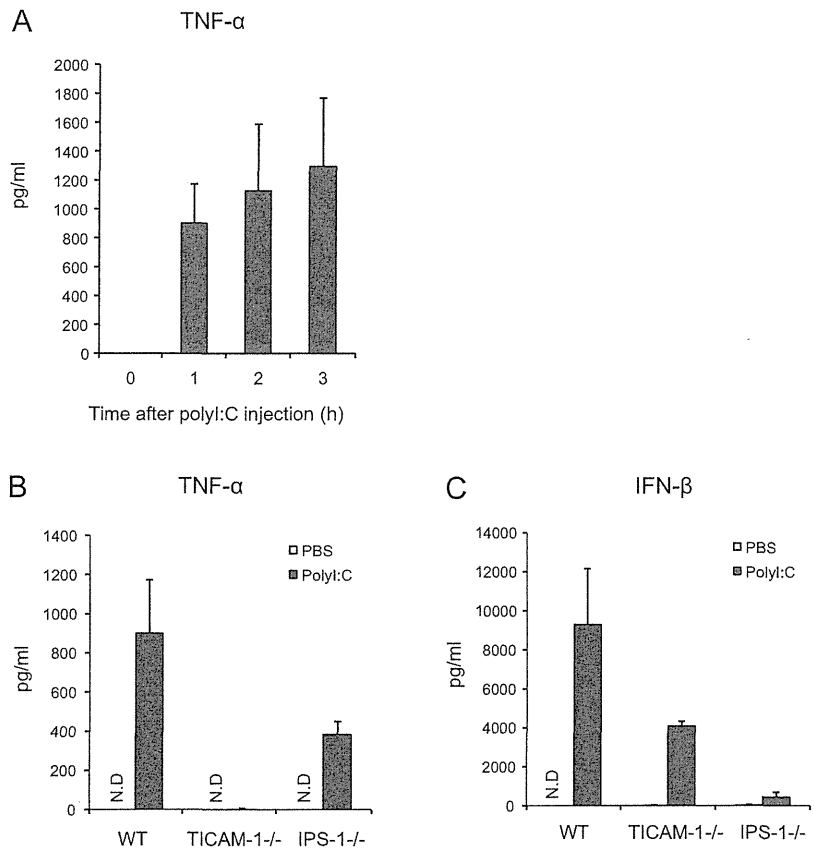


**Fig. S4.** Cytokine production in polyI:C-treated mouse. (*A*) WT mice were injected i.p with 200 μg polyI:C. After 0, 1, 2, and 3 h, TNF-α concentration in serum was determined by ELISA. (*B* and *C*) WT, TICAM-1$^{-/-}$, and IPS-1$^{-/-}$ mice were injected i.p with 200 μg polyI:C. After 1 h for TNF-α (*B*) and 4 h for IFN-β (*C*), serum cytokine levels were determined by ELISA. Data represents mean ± SD ($n$ = 3). N.D., not detected. A representative experiment of three with similar outcomes is shown.

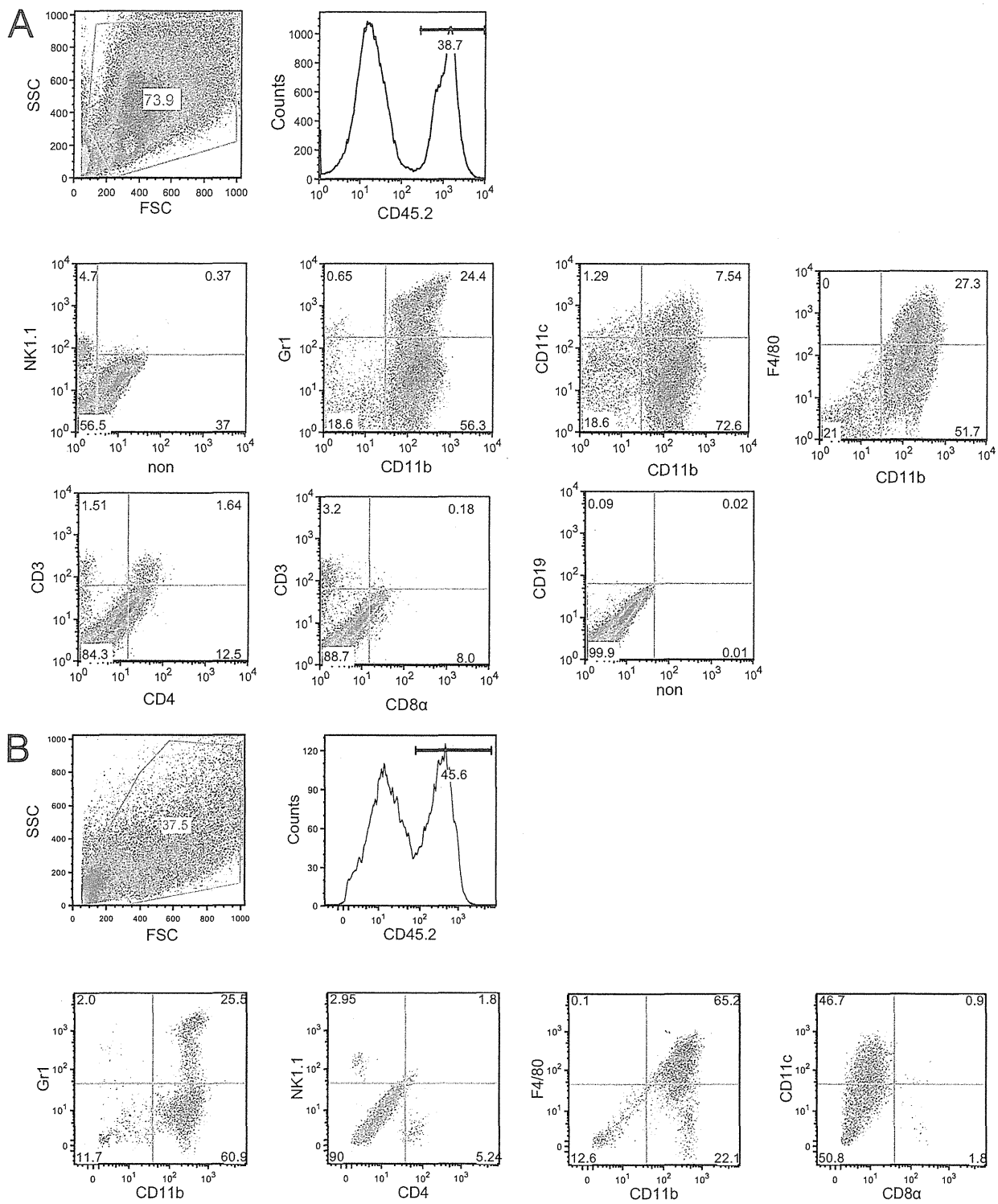


**Fig. S5.** Analysis of immune cells infiltrated into tumor. 3LL tumor cells ($3 \times 10^6$) (*A*) or MC38 ($1 \times 10^6$) (*B*) were transplanted s.c into B6 WT mice. After 2 wk, flow cytometric analysis was performed using freshly isolated whole tumor cell preparations in combination with staining of surface markers. $CD45.2^+$ cells were gated, and the expression of indicated surface markers was further analyzed. Numbers represent percentage of the gated and positive cells. A representative experiment of two with similar outcomes is shown. FSC, forward scatter; SSC, side scatter.